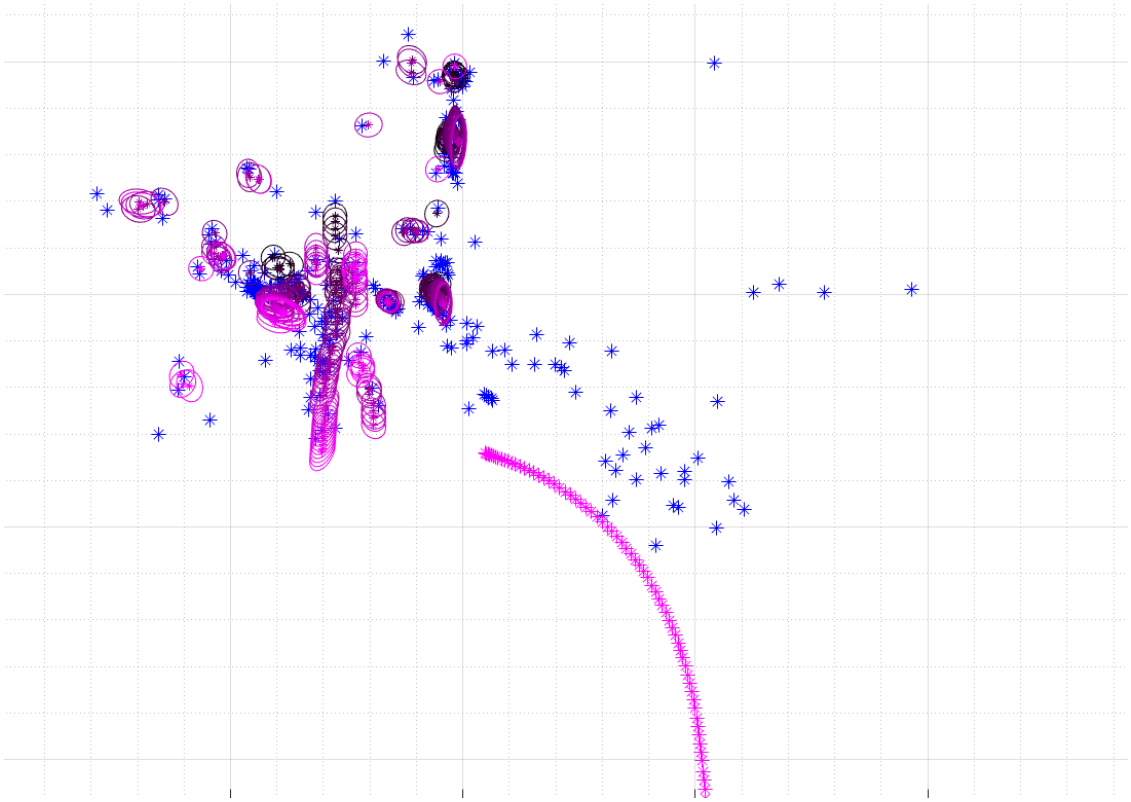

Tracking Stationary and Moving Extended Objects in Dense Urban Scenarios

An Application of the PMBM Filter with Stochastic Optimization to Radar Data

Master's thesis in Master Program Communication Engineering

GORKA ITURBE OTEGUI

Department of Electrical Engineering
CHALMERS UNIVERSITY OF TECHNOLOGY
Gothenburg, Sweden 2018

Master's thesis EX088/2018

Tracking Stationary and Moving Extended Objects in Dense Urban Scenarios

An Application of the PMBM Filter with Stochastic Optimization to Radar Data

GORKA ITURBE OTEGUI

CHALMERS
UNIVERSITY OF TECHNOLOGY

Department of Electrical Engineering
Division of Signal Processing and Biomedical Engineering
Signal Processing Group
Chalmers University of Technology
Gothenburg, Sweden 2018

Tracking Stationary and Moving Extended Objects in Dense Urban Scenarios
An Application of the PMBM Filter with Stochastic Optimization to Radar Data
GORKA ITURBE OTEGUI

GORKA ITURBE OTEGUI, 2018.

Supervisor: Johan Degerman, SafeRadar Research Sweden AB
Examiner: Karl Granström, Department of Electrical Engineering

Master's Thesis EX088/2018
Department of Electrical Engineering
Division of Signal Processing and Biomedical Engineering
Signal Processing Group
Chalmers University of Technology
SE-412 96 Gothenburg
Telephone +46 31 772 1000

Cover: Real urban scenario estimates when the car is approaching a crosswalk with a pedestrian moving on it.

Typeset in LaTeX
Printed by [Name of printing company]
Gothenburg, Sweden 2018

Tracking stationary and moving extended objects in dense urban scenarios
An application of the PMBM filter with stochastic optimization to Radar data
GORKA ITURBE OTEGUI
Department of Electrical Engineering
Chalmers University of Technology

Abstract

The problem of tracking dense urban environments to provide safety on the roads has always been of interest in the field of Autonomous Driving vehicles. Advances in the radar sensor technology have helped to tackle this problem, contributing to the Autonomous Driving systems with more robust and efficient solutions. Combining radar developments and mathematical theories like Finite Set Statistics and probability theory, this thesis employs and analyzes the performance of the Poisson Multi-Bernoulli Mixture filter with stochastic optimization when it is applied to Radar data. The results show that it is a robust approach that solves both real and simulated tracking problems in dense scenarios, and it is a suitable and compact method that tracks multiple kinds of objects found in urban scenarios.

Keywords: Autonomous Driving, dense urban scenario tracking, Poisson Multi-Bernoulli Mixture Filter, Multiple Hypotheses Tracking, Finite Set Statistics, Random Finite Set theory, Stochastic Optimization

Acknowledgement

I would like to thank first to my supervisor Karl Granström for his theoretical support, through both papers and meetings, and his guidance in the thesis understanding. I am also thankful for the help obtained from Johan Degerman, without whom I would not have advanced and learnt fundamental procedures employed in the actual vehicle Radar industry. I also want to thank Thomas Pernstal and SafeRadar Research Sweden AB for letting me use real data and their knowledge related to the Radar and Lidar sensors.

As for my relatives, I am glad and proud of being part of my family, whose help and support during my master allowed me to both pursue personal goals and grow in every possible way. Last, but not least, I would like to thank to all my friends in Göteborg, Bilbao and Stockholm for being supportive when it was more needed.

Gorka Iturbe Otegui, Gothenburg, August 2018

"Concern for man and his fate must always form the chief interest of all technical endeavors. Never forget this in the midst of your diagrams and equations." - Albert Einstein

Contents

List of Figures

Chapter 1

Introduction

The Autonomous Driving (AD) industry is being continuously improved by rapid developments and evolution in sensing and signal processing technologies. The history of the AD brings the reader back to the 80s when first rehearsals on self-driving vehicles, conducted by the NavLab, succeeded [19]. Not only the AD business itself contributed to the growth of this industry, but also related fields such as Defence and Military, with Radar and GPS applications, developed some of the necessary tools that enabled the development of the vehicle industry. Furthermore, in partnership with industry, academia has always provided both conceptual and theoretical support when it comes to find smart solutions to AD problems. One example is the self-driving bus that, under the Project S3 - Shared Shuttle Service, run at Chalmers University of Technology in May 2018; a multi-disciplinary researching project which pursued the development of both business and technology of the ADAS, Advanced Driver-Assistance Systems [18].

AD relies on the idea of adopting the behaviour of the driver, that is, replicating the human conduct on the road, to reduce the risk behind the existing interaction between human and vehicle as much as possible. Examples of this are new designs and implementations that equipped the AD vehicles with some of the tasks that drivers are facing each day in dense traffic situations, like line parking or cruise control.

Although the state of the technology can not always provide a means to execute advanced algorithms and ideas, the available sensor technology has let the ADAS industry grow and take fundamental steps towards safer autonomous vehicle driving, in part by tracking of the surroundings.

A technology that contributed to the growth of this AD business and holds also a particular importance in the scope of this project is the well-known radar sensor. It detects the range, velocity and heading information of an object through radio waves, making it possible to locate the object within a certain Field of View (FoV). It is worth noting that air surveillance, based strongly on the Radar sensor, contributed to the development of a crucial aspect studied in this thesis: the Multitarget Tracking (MTT) algorithm.

In addition, the resolution of the mentioned radar plays a decisive role in the development of the ADAS, where high resolution sensors allow the system to understand or perceive the nearby surroundings better. However, due to the high resolution radar, the Data Association (DA) analysis of all possible combinations of the available measurements with any of the multiple sources[1] within the FoV will be needed to be performed. Moreover, the assumption of small objects is no longer valid, since each of the detected objects might occupy several sensor cells. Therefore, the tracking requires a more exhaustive analysis based on extent or target shape tracking, rather than point based objects tracking [4].

This well-known difficulty behind the commented computational effort of the associations can be found in many extended target tracking publications [4][6][12][16], where methods such as Clustering and Assignment (C&A) are presented as solutions to the problem. However, these are not considered in this project [7], since they tend to fail when it comes to handle the detection of spatially closed objects [6]:

Therefore, new approaches based on solid mathematical grounds are to be derived to enable an efficient and robust multitarget filtering analysis.

[1] Also known as targets.

Chapter 2

Purpose, Objectives, Contributions and Ethics

Having introduced the multiple extended target tracking problem in which the thesis is centred around, in this forthcoming chapter, a deeper description of the MTT problem is first introduced and a short literature review about possible solutions is presented[1], followed by the aim of the thesis and motivating the selection with the objectives and contributions. The chapter ends with the ethics behind the project.

2.1 Multitarget Tracking Problem

The FoV around an AD vehicle needs to be characterized, tracking the different objects within. For instance, one could picture oneself as the ego-vehicle where the PMBM filter is mounted on, and look at the surroundings throughout some time interval. If the reader then checks and writes down the type of objects and the location in where they were seen, the analysis would end then in a list of multiple objects that crossed the view[2]. Moreover, the reader should take a further step, and notice how the brain classified the surroundings[3] which is the analogous to the main idea employed[4] in this project. The mentioned list of objects will be the output of this project filter, which could be used to take decisions like turn, stop or any other driving decision, as it is done by the driver.

[1]Note that due to the constant growth of the AD industry, many solutions are already out in the market; and since the coverage of all available solutions, also denoted as filters or trackers, is not feasible, the general filter families are given.

[2]Reader's FoV.

[3]With the help of the eyes, the radar in the ego-vehicle case.

[4]With a slightly different step called prediction.

Note in the commented example how the scan volume consisted of more than a single extended object, which demanded to our brain a thorough analysis on estimating what each thing within the FoV was. This same complexity, that the reader's brain processed, needs to be solved as efficient as possible and in the same manner as in the reader's brain; also known as MTT problem.

2.2 Multitarget Filters Survey

The previous dense FoV cluttered with different types of objects, such as stationary and non-stationary ones, should be estimated to ensure the safe operations of autonomous vehicles. Methods based on classical Bayesian inference (association and estimation) have given solutions to the tracking problem, which have also the adhered difficulty of processing in a tractable and efficient manner the DA [16] [4] [6].

Possible solutions to the MTT problem can be obtained analyzing different approaches described in the literature of the MTT filters, which [12] divides into three main groups explained in this next section. Note here that this tracking approach is based in a particular term called global hypothesis, which it refers to the derived probability that one possible combination of the available data takes, at same time step and after DA analysis.

Conventional Hypothesis-Oriented Filters

The Single-Hypothesis Correlation (SHC), Multi-hypotheses Correlation (MHC) or Composite-Hypotheses Correlation (CHC)[5] rely on the division and parallelization of the multitarget space, known as "divide-and-conquer" strategy. This approach allows MTT to be treated as multiple single target tracking problem. The following important assumptions have to be made in order to proceed with this hypotheses oriented approach[12].

1. The targets are either detected, missed or false-alarm signals and depend strictly on some empirical threshold. For further information, please refer to the explanations and figures in [12, p 289].
2. The targets are not extended nor unresolved.
3. At any time step, there exits a state estimate with its error estimate.
4. The motion of a target is uncorrelated to other target motion.

[5]Traditional methods in the multiple targets tracking problem.

Special attention is required in the second assumption where it is stated that the target must be of the form of point-target rather than of extended target. This collides with one of the main problems of this project, the extents of the targets, that will be addressed by approximating one of the following existing hypothesis-based tracking families.

SHC-based filters: At time step $k+1$, the set of N-hypotheses[6], describing the different unions of possible estimates of real targets and which are characterized by 3-tuples of the form of $\{(l^1_{k|k}, \mathbf{x}^1_{k|k}, P^1_{k|k}), ..., (l^N_{k|k}, \mathbf{x}^N_{k|k}, P^N_{k|k})\})$[7], turns into the $k+1$ time step prediction set. Right after, the association with the hypothesis with minimal association cost is chosen and measurement updates over these N-hypotheses are applied based on this calculated cost. This leads a unique hypothesis with the minimal cost to govern all the other hypotheses updates [12]. One single target filter that can be used within SHC-based family is the Kalman Filter. The procedure lays on processing multiple n-KF simultaneously, so independent hypotheses are obtained.

This minimum association cost might not correspond to the true association. Instead, [12] suggests another family of filters, the MHC, which are based in selecting multiple hypotheses[8] where the correct association might be hopefully presented. A downside is the complexity and computational cost, where *each* predicted hypothesis gives *multiple* hypotheses; each one describing a particular association of the data within the measurements set and bringing new possible scenarios into the analysis. That is the reason why this group is said to be part of the ideal solution, where every possible hypothesis is taken into account but impossible to be implemented due to its exponential increase.

To achieve tractability in MHC, approximations has to be made, to reduce the cost of the hypotheses computations. Throughout the literature different approximations are found to be the key; for instance, a threshold could be employed where the global hypotheses weights[9] are compared to the said threshold and the linked hypotheses prune if the commented weights do not reach the threshold [12]. Another approach, which does not use a probability threshold, is pruning less likely global hypotheses, until a particular number of them are obtained. That is, at

[6]Note here that *Single Hypothesis* is not directly related to the amount of targets, but to the minimal association cost.

[7]Where $l^n, \mathbf{x}^n$ and P^n stand for the n^{th}-hypothesis identity tag (an address or reference to find any hypotheses), estimate of the state and estimate error or covariance, respectively.

[8]Not only the one with minimum cost.

[9]Normalized probabilities describing the likelihoods of possible multiple targets estimates spaces or hypotheses.

each time step a pruning is done over all possible global hypotheses leaving the N^k most likely hypotheses. This approach allows to maintain a fixed amount of hypotheses[10], but it requires a decision step of selecting just a N^k amount of hypotheses. Both methods commented have been implemented and tried during the project, but due to computational efficiency, this last approach of fixed amount of global hypotheses was selected.

The CHC-based filter is a mixture of the previously described approaches. In this case, measurements, part of a set and related to any of the hypotheses, are weighed according to their degree of contribution to any of the hypotheses. These weighed measurements are rearranged to form "composite tracks"[11]. The Joint Probabilistic Data Association (JPDA) filter is a filter that belongs to the mentioned CHC-based filter group.

In this thesis, an MHC filter is used for MTT with extended targets.

2.3 The Purpose of the Thesis

2.3.1 Purpose: Tracking MTT problems by means of the Poisson Multi-Bernoulli Mixture Filter

A solution to the tracking problem presented in the Introduction section can be:

From the groups of methods commented in [6] that belong to the common approaches to solve the MTT problem, [12] proposes to employ Random Finite Set (RFS) approach. This theory that was formulated and committed only to mathematical purposes providing[12] *"a systematic toolbox [...] that addresses many difficulties - those involving ambiguous evidence, unification, and computation, especially", it is now employed to solve the MTT problem. In other words, the description of the dense FoV under analysis throughout a tractable and efficient filter will be obtained by joining the RFS theory, Poisson Point and Multi-Bernoulli Processes, with the Bayesian Inference; leading to an implementation of an efficient approximation MHC filter.*

[10] Computational efficient.

[11] The author uses tracks to refer to the commented hypotheses. In the case of this thesis, composite hypotheses.

[12] Claimed by [12].

2.3.2 Objectives and Contributions

Based on previous studies, [6], [7] and [8], the joint estimation of moving and stationary extended objects, throughout this thesis, will be aimed at:

1. The study of Bayesian Inference and Random Finite Set theory as a combined solution to multitarget filtering.
2. The use of particular instances of RFS theory such as Poisson Point and Multi-Bernoulli Processes to solve dense scenarios.
3. The employment of the Gamma Gaussian Inverse Wishart to describe any single extended target estimate.
4. The application of particular stochastic optimization applied to radar measurements, to reduce computational-costly DA algorithms.

and contributing with

1. The performance test of the filter under real scenario estimation.

2.4 Ethics: Trespassing Privacy - Awareness

In this section, I want to highlight the concern that technology must be always devoted to the development of both the human being and the society. Steps towards advanced techniques should be taken weighing the benefits and disadvantages of new inventions and ideas.

Trespassing Privacy and Awareness. Fundamental aspects about the field under analysis lays on the privacy and how it is handled. The aim of this thesis is to provide a detailed urban-landscape situation around an ego-vehicle, which might also include the tracking of the human being.

Being conscious about the Article 12 of the Universal Declaration of Human Rights of United Nations, that states:

No one shall be subjected to arbitrary interference with his privacy [...] Everyone has the right to the protection of the law against such interference or attacks.

the next point is claimed:

In accordance with the Article 12 of the Human Rights cited above, the forthcoming thesis, as well as, the project behind, is strictly based on providing an algorithm that allows to classify and shape any kind of objects[13] *within a specified area. Therefore, everything that goes beyond the use of the stated is not gathered or seen as part of this work, for this thesis. Main aim is focused on providing a safer environment for the human being.*

[13]Which includes the human being, but does not treat it differently in comparison to other objects within the FoV.

Chapter 3

Theory

The aim of this thesis is to track the environment around a reference vehicle, also known as ego-vehicle. These surroundings are modelled as "randomly varying numbers of randomly varying objects of various kinds"[12]. This statement defines accurately the purpose of this work, but also arises difficulties when well-established filtering theories and assumptions are employed, such as single target Bayesian filtering.

Since the sources, from which the estimations are made, might be of various kinds and numbers, the complexity will be also increased in terms of data handling and association, making some estimation methods not suitable under some specific given circumstances. In this project, the high resolution radar makes the point-target assumption to be not held anymore. Hence, single target filters, based in the previous supposition, do not work any longer for the extended object tracking.

Analogous to the example given in [12, p. 16], the objects entering the FoV of a vehicle can be assumed, in a sensible manner, to join the space randomly; like in the well-known queuing theory. Since the location of these objects do not need to be deterministic, the randomness in all target-positions must be introduced into the estimation, which [12] describes as "Multidimensional Point Process". The shape might also change in form, which in the instance of this work does not occur, and in that case it could be in a non-deterministic way. However, it might be worth considering in other cases such as group tracking algorithms [6].

In this thesis, we will employ a filter named Poisson Multi-Bernoulli Mixture, PMBM. It is an adaptation of the conventional Bayesian Inference to the Finite Set Statistics Theory, FISST, where real situations are intended to be represented as accurate as possible. Moreover, since a sensible way to describe the limited knowl-

edge about the space around the vehicle is sought, the employment of Random Finite Set (RFS) theory, part of FISST, becomes a natural choice [4].

The real application of the theory gets visible when one refers to its existing implementation such as the Probability Hypothesis Density (PHD), Cardinalized PHD (CPHD) or the one employed throughout this project. The previous first two filters can be said to be characterized by the concept of sufficient statistics, which enable to compress the posterior to the first couple of moments. High SNR (Signal-to-Noise Ratio) must be assumed, which provides a way to derive the posterior probability distributions, *pdf* [11]. These approaches differ from the studied one in the facts that they firstly group-track the environment (a formation of targets that share a common motion [4]) and they continue with individual target tracking [12]. Also, no assumption of high SNR is made upon the PMBM filter.

Lastly and worth emphasizing[1], the real applications of the mathematical foundations or algorithms are done throughout the employment of models, which simplify the abstraction of the mathematical approaches up to large extent. The selection of models is the key factor then, when it comes to build solid filters that provide trustworthy estimates that make possible future decision/control steps safer. The construction of strong and stable filters with suitable models is a fundamental part in which ADAS are built on and hence studied throughout this project.

3.1 The Bayesian Approach for Single Target Tracking

Intended to an audience that should have already some knowledge about object tracking or filtering, a good introductory point for this thesis lays on the Kalman filter (KF). It is a particular case of single-target tracking based on Bayesian Inference, which becomes helpful for understanding the PMBM filtering procedure.

Basically, the Kalman filter predicts the k-time step sequence state from a previously estimated sequence state, comprising state estimates such as position, velocity and/or any other describing parameter. Alongside with this sequence state estimation, a corrector is presented, with the uncertainty of the calculated state estimate. The KF corrects this state by means of measurements, collected by either one or more sensors. It is important to notice that every tracking problem needs

[1] Commented and rephrased directly from [12].

an initialization state, also called prior knowledge, defining the initial conditions. In other words, the prediction step equations, containing both the prior estimated sequence state and its uncertainty, will be of the form of

$$\hat{\mathbf{x}}_{k|k-1} = F_k \hat{\mathbf{x}}_{k-1|k-1} \tag{3.1}$$

$$P_{k|k-1} = F_k P_{k-1|k-1} F_k^T + Q_k; \tag{3.2}$$

while the update step of the predicted sequence step will be based in

$$\mathbf{y}_k = \mathbf{z}_k - H_k \hat{\mathbf{x}}_{k|k-1} \tag{3.3}$$

$$S_k = R_k + H_k P_{k|k-1} H_k^T \tag{3.4}$$

$$K_k = P_{k|k-1} H_k^T S_k^{-1} \tag{3.5}$$

$$\hat{\mathbf{x}}_{k|k} = \hat{\mathbf{x}}_{k|k-1} + K_k \mathbf{y}_k \tag{3.6}$$

$$P_{k|k} = (\mathbf{I} - K_k H_k) P_{k|k-1} (\mathbf{I} - K_k H_k)^T + K_k R_k K_k^T. \tag{3.7}$$

$$\tag{3.8}$$

So, the procedure by which the Kalman filter is addressed may be summarized briefly with initialization, prediction and correction steps. These state-sequence-estimating equations can be rewritten with general probability density functions through Bayesian Inference, as it is shown in [12] [4] [6]. As it will be shown later, the procedure to return to the equations will lay on employing a well-known *pdf*.

Before digging into the mentioned Bayesian approach, recall the theory that allows to proceed with the state-sequence-estimating descriptor, the Markov Chain, and which represents a key factor in the prediction step. In the employed first order Markov model, the previous sequence state estimate and only this, identified as $\hat{x}_{k-1}$, is used to predict the next state estimate; discarding previous ($[t] = K, ..., k-2$) time steps from the $[t] = k$ prediction stage. In the end, the sequence can be seen as states that are linked solely by previous time steps, literally like in a chain.

Following the derivations shown in [12] and to reduce the length of this thesis, the prediction and correction steps, after some manipulations, lead to the following definitions based merely in probability distributions[2]; which are the generalized cases of the previously explained KF equations. As for the prediction, one could

[2]Following the definitions, example distributions are also given so that the reader can understand the ideas behind better.

express it with the generalized form as

$$f_{k+1|k}(\mathbf{x}) \triangleq \int f_{k+1|k}(\mathbf{x}|\mathbf{x'}) \cdot f_{k|k}(\mathbf{x'}|\mathcal{Z}^k)\, d\mathbf{x'} \tag{3.9}$$

$$\overset{\text{example}}{=} \int \mathcal{N}_{Q_k}(\mathbf{x} - F_k\mathbf{x'}) \cdot \mathcal{N}_{P_k}(\mathbf{x'} - \mathbf{x}_{k|k})\, d\mathbf{x'}; \tag{3.10}$$

and the update step as

$$f_{k+1|k+1}(\mathbf{x}) \triangleq \frac{f_{k+1}(\mathbf{z}_{k+1}|\mathbf{x}) \cdot f_{k+1|k}(\mathbf{x}|\mathcal{Z}^k)}{\int f_{k+1}(\mathbf{z}_{k+1}|\mathbf{y}) \cdot f_{k+1|k}(\mathbf{y}|\mathcal{Z}^k)\, d\mathbf{y}} \tag{3.11}$$

$$\overset{\text{example}}{=} \frac{\mathcal{N}_{R_{k+1}}(\mathbf{z}_{k+1} - H_{k+1}\mathbf{x}) \cdot \mathcal{N}_{P_{k+1|k}}(\mathbf{x} - \mathbf{x}_{k+1|k})}{\int \mathcal{N}_{R_{k+1}}(\mathbf{z}_{k+1} - H_{k+1}\mathbf{y}) \cdot \mathcal{N}_{P_{k+1|k}}(\mathbf{y} - \mathbf{x}_{k+1|k})\, d\mathbf{y}}. \tag{3.12}$$

From example equations 3.10 and 3.12, some conclusions can be drawn. Notice the sub-indexes used for the Normal distribution notation, representing the covariances of each of the steps at a particular time. Remember that any Gaussian *pdf* can be described in terms of its mean and covariance.

Now, if the prediction step is unfold, two basic ideas related to the prior $\mathcal{N}_{P_k}$ and the transition $\mathcal{N}_{Q_k}$ distributions can be seen. The $\mathcal{N}_{P_k}$ *pdf* is directly pointing to the prior knowledge of the system at some specific time, with the particularity of holding a P_k uncertainty within. The $\mathcal{N}_{Q_k}$ one, in eq. 3.10, is linked to the transition function or explained process model, F_k in the example, which is characterized with a particular uncertainty known as process noise Q_k. Thus, from the prior knowledge, $\mathbf{x}_{k|k}$, the prediction function, $f_{k+1|k}$, is obtained and it represents new possible sequence states and the uncertainties with a *pdf*.

The correction step, which is normalized in the shown case and gives the exact correction expression $f_{k+1|k+1}$, can be understood as the corrector of the calculated prediction. The information derived from the prediction step is saved in the $f_{k+1|k}(\mathbf{x}|\mathcal{Z}^k)$ and scaled to the the factor $f_{k+1}(\mathbf{z}_{k+1}|\mathbf{x})$. This simple idea will adapt the prediction information with the obtained measurements from the sensors; giving as a result a more reliable and narrowed outcome.

As it has been shown, the KF equations and the commented distributions describe the same underlying idea, this is, an iterative estimating/filtering procedure. The well-known distribution commented before that translates the generalized Bayesian Filtering into the KF equations is the linear Gaussian distribution, shown in eq.3.10 and eq.3.12.

Now, recall that the KF is only valid under some specific conditions[3] and unfortunately non-linearities and sudden changes in the real world are not considered in the the model. Consequently, the KF gets discarded for only supporting single non-extended targets and not representing the final aim of this thesis, a multitarget tracking system. This problem can be handled by employing multi-variable analysis based on Bayesian Inference, but it often requires time-consuming mathematical procedures. Several tools that are accessible from the signals processing theory can alleviate this long procedures[4] such as the moment generating function or probability-generating functional.

3.2 Random Finite Sets: General Point Processes and Poisson Point Process

The RFS theory is the foundation on which the PMBM filter is based and that contains the following two characteristics: the event space and intensity [17][5]. This chapter is focused on explaining briefly the general point process and the particular Poisson Point Process (PPP) within the RFS theory. Note that some knowledge about random variables, processes and topology is required for the following section.

3.2.1 The Event Space

Assume a class of random sets of which realizations are in the state space $\mathcal{S}$. Assume also that $\mathcal{S}^\infty$ is the hyperspace of all finite sets of $\mathcal{S}$ that includes the empty space within, $\mathcal{S}^\infty \cup \emptyset$. The sets that inherit the nature of the finite hyperspace, $\boldsymbol{\Psi} \in \mathcal{S}^\infty$, will be then known as a Random Finite Set (RFS)[6]. For example, if the process inside the RFS is independent and identically distributed with the Poisson distribution, then it is identified as the well-known PPP.

Assume now that the $\mathcal{S}$ state space is the Euclidean space $\mathbb{R}^d$, $d \geq 1$. This derives from the fact that the AD problem is suitably parameterized by the Euclidean space, since the surroundings of any vehicle can be expressed in terms of Euclidean

[3] Linear transition models, for instance.

[4] Multi-variable derivatives and integrals which transform single variable analysis into multiple variable analysis.

[5] Further information about these Random Processes, Point Processes and Topology theories can be found throughout the literature, for example, in [12], [13] and [10].

[6] Also denoted as random set.

Canonical Coordinates[7]. If at a given k-time step the process contains a limited number of points, $n \in \mathbb{N}$, and states $\mathbf{y}_i \in \mathbb{R}^d \,|\, i \in [1, n]$, then the random set $\mathbf{\Psi}$ can be parameterized as

$$\mathbf{\Psi}^k = \{\mathbf{y}_1^k, ..., \mathbf{y}_n^k\}. \tag{3.13}$$

Note that the general process above describes a set, thus no ordering or listing is applied into the elements. For notational coherence with the employed reference, the state space will be denoted as $\mathfrak{X}$ and the measurement space as $\mathfrak{Z}$. Hence, within the scanned FoV, $\mathbb{R}^d$, there exists always a random set describing a group of targets or objects and another random set describing a group of measurements as

$$\exists \mathbf{\Psi}^{\texttt{Targets}} \in \mathfrak{X}^\infty \text{ and} \tag{3.14}$$
$$\exists \mathbf{\Psi}^{\texttt{Measurements}} \in \mathfrak{Z}^\infty. \tag{3.15}$$

Instantiations of these random sets will give the k-time step

$$\mathbf{\Psi}^k_{\mathfrak{X}^\infty} = \mathcal{X} \text{ and} \tag{3.16}$$
$$\mathbf{\Psi}^k_{\mathfrak{Z}^\infty} = \mathcal{Z} \tag{3.17}$$

Hereafter, the k could be dropped from the set notation if not required, due to notational simplicity and brevity.

3.2.2 Intensity

As it can be found in the studied literature, the PPP is parameterized by a function called intensity, henceforth denoted by D. It describes the level of concentration of the process point under analysis in any subset of $\mathcal{S}^\infty$. Following [6], the intensity with two parameters: the rate $\lambda > 0$, sampled from a Poisson distributed random set, and the spatial state, modelled by sampling a space distribution f, for instance, a Gaussian Normal distribution. As a result, the intensity takes the expression of

$$D = \lambda \cdot f. \tag{3.18}$$

[7]The necessary orthonormal base upon which any object can be built and represented algebraically within a space.

Worth noticing is that the integral of the intensity upon any subset of the finite hyperspace set $\mathcal{S}^{\infty}$ will point to the expected number of members of the subset [6].

3.3 Multitarget Measurements

Revisiting the KF due to the simplicity and familiarity that offers when it comes to the analysis of the single target filter problem, the measurement likelihood function for a single target can be described. As it was also done previously, the underlying Bayesian Inference will be the procedure on which the forthcoming technique is built.

The Bayesian Inference for single target filtering can be employed to obtain the measurement likelihood if the equation under analysis is of linear/non-linear and additive nature. Then, the likelihood can be written as

$$f_{k+1}(\mathbf{z}|\mathbf{x}) = \mathcal{N}_{R_{k+1}}(\mathbf{z} - \eta_{k+1}(\mathbf{x})) \tag{3.19}$$

$$\eta_{k+1}(\mathbf{x}) : \text{The nonlinear/linear measurement model of the KF.} \tag{3.20}$$

Several mathematical manipulations and deductions have been assumed above, which can be found in [12].

Now, given the single target likelihood function and the random finite set theory, the concept of measurement set likelihood can be introduced. As shown before, the most convenient notation, to most of the AD problems and for both target states and measurements, is given by a set nomenclature; representing a dynamic and disarranged group of targets inside the FoV state space,

$$\mathcal{X} = \{\mathbf{x}_1, ..., \mathbf{x}_n, ..., \mathbf{x}_N\} \text{ where } n \in \{1, ..., N = |\mathcal{X}|\} = \mathbb{I} \text{ and} \tag{3.21}$$

$$\mathcal{Z} = \{\mathbf{z}_1, ..., \mathbf{x}_m, ..., \mathbf{z}_M\} \text{ where } m \in \{1, ..., M = |\mathcal{Z}|\} = \mathbb{M}. \tag{3.22}$$

A more thorough look at the set describing the measurements of the FoV will show that the set is of multiple kinds; where both measurements from actual objects, false alarms and clutter are found within the set $\mathcal{Z}$.

In what it follows, the union of different measurement sources is presented. Within the set, different situations can be studied such as no target is presented, a target is presented or an expected target within the field is missed. Note that these previous conditions are disjointly unified in the $\mathcal{Z}$ measurement set since

they are independent from each other and also that sudden events can end in empty outputs or measurements, for instance, an interruption in the sensors data collection process at some k-time step. Hence, let the disjoint measurements set or union of different collected measurements be written as

$$\mathcal{Z}_k = \Upsilon(\mathcal{X}_k) \uplus C_k = \Upsilon(\mathbf{x}_k^1) \cup ... \cup \Upsilon(\mathbf{x}_k^n) \uplus C_k, \text{ this is,} \tag{3.23}$$

$$\text{Measurement set} = \text{Collected measurements set} \uplus \text{Clutter set.} \tag{3.24}$$

3.3.1 Object Classification in Terms of FoV

Occluded objects: In the case of undetected objects, the reader might naturally assume that the scene is an "empty" space just composed by clutter measurements. This assumption is not valid for this project, motivated by the necessity of describing the FoV as faithfully as possible. For example, picture that the AD vehicle is on the road and at some instant some close trees or vehicles shadow people or cars that are also within the field. In the case of such event, it would be useful to represent in the filter the objects that may exit, but were not detection. To do this, the PPP is useful.

As common as the previous non detected targets FoV are the detected targets environments. These objects can be classified in different ways, but if [4] is followed, a differentiation in the nature of the targets can be found: new targets entering into the FoV and targets that were previously and still continue to be in the scan area.

A new target might become visible to the sensor field at some random point of the tracking sequence. This event triggers the sensor and introduces measurements together with clutter. However, the one target/object scenario is not a common situation, due to the fact that most urban landscapes gather several targets within a specific area or volume.

Multiple targets are presented: If a target was already within the FoV, which most certainly will happen for a certain amount of time steps during the driving time, the filter will locate the presence and shape it accordingly. The estimates should get more stable and precise with time where no sudden changes happen. Similar to single target filters, the PMBM filter will allow to individually but group wise[8] analyze the targets or tracks inside the scanning area or volume.

[8]It might seem a paradox to be possible to analyze individually but in a collective way, but the reader should notice that the PMBM filter gives an overall outcome with specific details of each of the targets within the FoV, in other words, a fully described multitarget scenario.

Missed detection: Assume that the presence of an object is still within the scanning area in the next time step under analysis. Now, picture a sudden external factor affecting the performance of any of the sensors mounted on the AD vehicle. The existence of a target is known, but the tracking might have been affected partly or fully by the loss of the associated measurement(s). This event is not unusual, since randomness can be found in the components of the ADAS. The filter is provided with a method to deal with this kind of situations; a procedure that corrects the prediction without any associated measurement(s).

3.3.2 Multi-sensory Vehicles

The case of multisensor space can be also investigated, but since the sensor are assumed to be uncorrelated in their measurements, the disjoint sets are equally represented within an only k-time step $\mathcal{Z}$ measurements set that contains all measurements from all possible sensors. That is,

$$\mathcal{Z} = \{\overset{1}{\mathcal{Z}} \uplus \overset{s}{\mathcal{Z}} \uplus \overset{S}{\mathcal{Z}}\} \text{ where } s \in S \text{ (The } S \text{ group or set of sensors).}$$

3.3.3 Measurement Likelihood

Recalling that the measurements inside the $\mathcal{Z}$ set are independent from each other, the next likelihoods describing clutter or targets clustered scenarios are introduced. Important probabilities to take into account when these likelihoods are calculated are the survival and detection probabilities, since they play fundamental roles in the presence and lifespan of any object within the FoV.

Imagine that a prediction is to be made about an object inside the FoV. It is highly likely that an object might end up outside from the scanning space of the sensors at some point of the tracking sequence. This probability of remaining inside or outside is captured by p_S, the probability of survival. Now, depict another scenario where the occurrences are always given inside the FoV, but that might be undetected due to external factors. For example, imagine the case that at the correction stage an object (previously tracked) is not detected. The probability assigned to this event is the probability of detection p_D, which is applied accordingly to all the objects within the FoV.

Recall what it is stated in [12] and [6] about independent and identical distributions. They are mathematically defined by

$$f(\mathcal{X}) \triangleq n! \cdot p(n) \cdot f(\mathbf{x}_1) \cdot ... \cdot f(\mathbf{x}_n). \tag{3.25}$$

Now, to the most of the purpose of shaping the undetected targets in a sensible manner and in this particular project, the def. 3.25, by means of Poisson distribution, $p(n)$, with rate λ, derives into the following density, after some manipulations and reductions,

$$f(\mathcal{X}) = e^{-\lambda} \cdot \lambda^n \cdot f(\mathbf{x}_1) \cdot ... \cdot f(\mathbf{x}_n) \tag{3.26}$$

$$= e^{-\lambda} \prod_{\mathbf{x} \in X} \lambda f(\mathbf{x}). \tag{3.27}$$

Employing the definition above, def. 3.25, with the particularity of Poisson distributed elements, eq. 3.26, the undetected targets get represented in a compact way.

As for the detection, the clutter (state independent) and the corresponding whole $\mathcal{Z}$ set likelihood (state dependent) are modelled [6] as

$$\kappa(\mathbf{z}) = \lambda c(\mathbf{z}) = \frac{\lambda}{A} \text{ and} \tag{3.28}$$

$$\ell_{\mathcal{Z}}(\mathbf{x}) = p_D(\mathbf{x}) e^{-\gamma(\mathbf{x})} \prod_{\mathbf{z} \in \mathcal{Z}} \gamma(\mathbf{x}) \phi(\mathbf{z}|\mathbf{x}), \text{ respectively;} \tag{3.29}$$

and where each product of the set likelihood that points to each measurement likelihood is proportional to the previously explained intensity concept described as

$$D^{\mathbf{z}} = \gamma(\mathbf{x}) \phi(\mathbf{z}|\mathbf{x}).$$

Note that A represents the specific volume the FoV is occupying and the pair γ and ϕ represent Poisson rate and spatial distributions at any time step, respectively. If a specific spatial distribution is introduced, such as the Normal distribution, then the spatial distribution of one measurement at k-time step is

$$\phi(\mathbf{z}_k|\mathbf{x}_k) = \mathcal{N}(\mathbf{z}_k; H_k \xi_k,\, X_k) = \mathcal{N}_{X_k}(\mathbf{z}_k - H_k \xi_k(\mathbf{x}_k)); \tag{3.30}$$

where H and ξ are the linearized measurement model and the state representation vector, respectively.

3.4 Modelling

The modelling of the environment around an AD vehicle is of high relevance, since it will improve the way the filter employs the available information. A good model

can be difficult to achieve if the transition or movement of the object is intricate; but if obtained, it will help to provide a solid estimate. As it is cited in [12], any algorithm supports all the necessary theoretical base to build a filter, but it can be tedious as a result of difficult and long mathematical derivations. Moreover, the motivation of using models is not only committed to the previous reason, but also to the better description of any physical phenomenon.

Different models are to be introduced into the filter, with particularities in their choices. As it has been explained, the pure mathematical approach will be reduced to a more compact and meaningful expression and a complete single target model is going to be defined.

3.4.1 Objects Classification in Terms of their Nature

In order to introduce a suitable model into the PMBM filter, an examination on the nature of the components forming the FoV should be done. As it is already said, a model will provide a physical description of the object of interest, hence the importance of it. In this project, the objects are either stationary such as vegetation/static landmarks or non-stationary such as moving vehicles, people or any kind of object in motion.

The election of these previous classes are not a requirement imposed by the PMBM filter, but these two commented kinds of objects represent in close form and sensible manner the surroundings of an ADAS. The way to classify the objects transitions will be obtained throughout assumptions upon a single and particular model, but other approaches such as the Interactive of Multiple Model (IMM) method are available in the literature and they might perform better than the studied one[9].

3.4.2 Kinematics or Motion Models

Assume that the commented moving and stationary objects are based on Constant Velocity (CV) model. It is clear that this assumption will arise problems when some motions[10] inside the FoV are required to be characterized. For instance, imagine the next urban landmark: several vehicles are on the road and within the FoV. At some time during the AD tracking, one/few of these objects might suddenly change its/their route/s with a particular turning. Although this can not be represented by the CV model since it lays on the assumption of straight

[9] IMM does work with more than a single model.
[10] Turnings, for example.

and constant velocity movement, the CV motion model will be, for considerable number of scenarios in this thesis, a suitable approach to describe objects within the FoV.

From a moving object, which is modelled by the CV model and after some assumptions, one can derive the motion model for the stationary object. Now, picture the following scenario: an AD vehicle is surrounded by vegetation, road rails, or a line of parked vehicles. It can be seen with some broad view that the CV motion itself implies the null movement of an object in its nature, this is, $\mathbf{v} = \mathbf{0} \in \mathcal{V} = \{\mathbf{0}, \mathbf{v}_1, ..., \mathbf{v}_K\}$. This can be acquired by a "zero"-CV model supposition, which all objects inside the FoV share. If the velocity in the space state estimate converges to zero, $\mathbf{v} \to \mathbf{0}$, then one can assume that the object under analysis is standing still. This approximation converges further when several time step are run over the same objects with no sudden changes.

3.4.3 Extent

The point based tracking exploits the relation of one-point-one-target, nut it becomes unsuitable in the sensors near field. Each object in an urban scenario can certainly cause more than a single point and in that case it is described by a cloud/collection of measurements. This idea of giving shape to what it is inside the FoV is known as extent, aimed at describing the shape and size of any target. Since one of the main aspect of any tracking filter is to provide to the decision step with all the necessary information about the features of the objects, it is a property that has to be calculated.

In the literature, [4] or [6] for instance, different approaches to solve these extensions are given. This project could be upgraded by implementing additional methods apart from the one selected, the Inverse Wishart Random Matrix [3] [9], taking, for example, rectangular shapes instead of elliptical ones[11]. However, the approach of elliptical shapes allows the employment of Gaussian distributions, hence reducing the computational cost just to the calculation of the mean and covariance parameters of a Gaussian distribution.

Algebraically, the Random Matrix can be understood as a symmetric and positive definite matrix of dimensions $d \times d$ that describes an elliptical shape, this is, $X_k \in S^d_{++}$; where d takes the dimensions of $\mathbb{R}^2$ or $\mathbb{R}^3$.

[11] Which describe much sensibly the vehicles shapes.

3.4.4 Space State Representation

Up until now, several aspects about the project have been introduced and explained: the classification of the FoV is now known to be partially described by the PPP; each object within this space is also known to be part of either a stationary or non-stationary class; the transition model is set to the common CV model and the likelihoods of the measurements set[12] have been examined. Therefore, the space state that belongs to any of the possible objects at any time step can be now written down within the commented Euclidean space using the Cartesian Coordinate system and the specific parameters of the PPP, rate and extension.

Setting the Euclidean space to $d = 2 \rightarrow S^2_{++}$, the state representation derives then into

$$\xi_k = \begin{Bmatrix} \gamma_k\text{: representing the Poisson Point Process} \\ \mathbf{x}_k \text{ :representing the state estimate} \\ X_k \text{ :representing the extension} \end{Bmatrix}, \tag{3.31}$$

where

$$\mathbf{x}_k = \begin{bmatrix} x_k \\ y_k \\ vx_k \\ vy_k \end{bmatrix}. \tag{3.32}$$

Note that eq. 3.31 is formed by three different properties of any of the objects within the FoV, where the introduction of the extension into the state representation describes a non classical filtering procedure. This leads to the solution of one of the project aims: the objects shapes.

3.4.5 The Single Extended Object Model: The Gamma Gaussian Inverse Wishart ($\mathcal{GGIW}$)

Following the suggestion of [4] and [6], a specific model to solve the problem of a single extended object using the ξ object space state representation and measurements space information is employed. This model, which will be introduced to the general filter scheme (section 3.5), is the Gamma Gaussian Inverse Wishart ($\mathcal{GGIW}$).

[12] Both clutter and target generated measurements.

Representing faithfully the reality around the vehicle together with computational efficient algorithms is of high importance and thus the conjugate prior is employed. Selecting the initial prior as a conjugate prior allows to describe any k-time step prediction and update steps with few same parameters. Furthermore, the usage of a PMBM conjugate prior based on RFS theory will also enable to describe separately undetected targets from detected ones [4][6] and parameterized the density model of interest.

Therefore, the parameters[13] that form the model are

$$\begin{aligned} \zeta_{k|k} = \zeta &= \{\alpha_{k|k}, \beta_{k|k}, \mathbf{m}_{k|k}, P_{k|k}, v_{k|k}, V_{k|k}\}, && \text{if} \quad k|k \\ \zeta_{k+1|k} = \zeta_+ &= \{\alpha_{k+1|k}, \beta_{k+1|k}, \mathbf{m}_{k+1|k}, P_{k+1|k}, v_{k+1|k}, V_{k+1|k}\}, && \text{if} \quad k+1|k \end{aligned}$$

where

$$\begin{aligned} \alpha \text{ and } \beta: &\ \text{Parameters of the Gamma distribution} && \rightarrow \mathcal{G} \\ \mathbf{m} \text{ and } P: &\ \text{Parameters of the Gaussian Normal distribution} && \rightarrow \mathcal{G} \\ v \text{ and } V: &\ \text{Parameters of the Inverse Wishart} && \rightarrow \mathcal{IW}. \end{aligned}$$

Each of the parameters commented above needs to be classified mathematically, found in [6] and [4], which they are defined as

$$\zeta_+ = \begin{cases} G & = \nabla_\xi\, g(\xi)|_{\xi=\mathbf{m}} \\ M(\mathbf{m})(\text{CV}) & = 1_{d\times d} \\ \alpha_+ & = \frac{\alpha}{\eta} \\ \beta_+ & = \frac{\beta}{\eta} \\ \mathbf{m}_+ & = g(\mathbf{m}) \\ P_+ & = GPG^T + Q \\ v_+ & = 2d + 2 + e^{\frac{-T_s}{\tau}}(v - 2d - 2) \\ V_+ & = e^{\frac{-T_s}{\tau}} M(\mathbf{m}) V M(\mathbf{m})^T \end{cases} \quad \text{and } \zeta \ = \begin{cases} \alpha & = \alpha_+ + |\mathcal{Z}| \\ \beta & = \beta_+ + 1 \\ \mathbf{m} & = \mathbf{m}_+ + K\epsilon \\ P & = P_+ - KHP_+ \\ v & = v_+ + |\mathcal{Z}| \\ V & = V_+ + N + Z \end{cases} \tag{3.33}$$

[13] In case more information is needed about the distributions of these parameters, direct to Mathematical Handbooks - Probability density functions - Conjugate Priors, Inverse Wishart, Gamma functions and Gamma distributions.

The complementary equations to the set of eq.3.33 are

$$g(\mathbf{x}) = \begin{cases} x_{k+1} &= x_k + \mathrm{v}_k^x T_s \\ y_{k+1} &= y_k + \mathrm{v}_k^y T_s \\ \mathrm{v}_{k+1}^x &= \mathrm{v}_k^x \\ \mathrm{v}_{k+1}^y &= \mathrm{v}_k^y \end{cases}; \qquad G = \begin{bmatrix} 1_{d\times d} & T_s * 1_{d\times d} \\ 0_{d\times d} & 1_{d\times d} \end{bmatrix}; \qquad H = \begin{bmatrix} 1_{d\times d} & 0_{d\times d} \end{bmatrix} \tag{3.34}$$

$$\begin{cases} \bar{\mathbf{z}} &= \frac{1}{|\mathcal{Z}|}\sum_{\mathbf{z}^i\in\mathcal{Z}_k}\mathbf{z}^i \\ Z &= \sum_{\mathbf{z}^i\in\mathcal{Z}}(\mathbf{z}^i-\bar{\mathbf{z}})(\mathbf{z}^i-\bar{\mathbf{z}})^T \end{cases} \qquad \begin{cases} \hat{X} &= \frac{V_+}{v_+-2d-2} \\ N &= \hat{X}^{\frac{1}{2}} S^{\frac{1}{2}} \epsilon\epsilon^T S^{-\frac{T}{2}} \hat{X}^{\frac{T}{2}} \end{cases} \tag{3.35}$$

$$\begin{cases} \epsilon &= \bar{\mathbf{z}} - H\mathbf{m}_+ \\ S &= HP_+H^T + \frac{\hat{X}}{|\mathcal{Z}|} \\ K &= \frac{P_+H^T}{S}. \end{cases} \tag{3.36}$$

and a single target likelihood of

$$\ell = (\pi^{|\mathcal{Z}|}|\mathcal{Z}|)^{-\frac{d}{2}} \frac{|V_+|^{\frac{v_+-d-1}{2}}\Gamma_d(\frac{v-d-1}{2})|\hat{X}|^{\frac{1}{2}}\Gamma(\alpha)(\beta_+)^{\alpha_+}}{|V|^{\frac{v-d-1}{2}}\Gamma_d(\frac{v_+-d-1}{2})|S|^{\frac{1}{2}}\Gamma(\alpha_+)(\beta)^{\alpha}}. \tag{3.37}$$

Equations above represent the $\mathcal{GGIW}$ in its whole for the Random Matrix approach, this is, for objects shapes approximated by ellipses. The fundamental parameters, shown in the set of equations 3.33, describe all the variables to describe any object inside the FoV.

Although all the equations presented are of relevance to the good performance of the PMBM filter, special emphasis on the likelihood (ℓ), eq. 3.37, is here highlighted due to the importance it holds in the stochastic optimization applied to the Radar data.

3.5 Multitarget Analysis

The multitarget tracking scenario is a dense environment where entering/leaving/occluded objects or targets can be found. This FoV can be described with an union of these different types of objects[14] [12] as

$$\mathcal{X}_{k+1|k} = \Gamma(\mathcal{X}_k) \cup B(\mathcal{X}_k) \cup B^{\mathrm{s}} \tag{3.38}$$

$$\text{Prediction set} = \text{Persisting set} \cup \text{Spawned set} \cup \text{Spontaneous set}. \tag{3.39}$$

[14] One could use a similar approach used when the measurements set was introduced to understand this following section.

Eq. 3.38 describes the different sets of objects that at some k-time step might have existed inside the AD surroundings. Any previously detected target might persist, spawn new set of births or disappear from the scanning area/volume in the next time step. Therefore, among all possible examples that fit in this union, eq. 3.38, the general case containing both target deaths and births has been chosen to be the one representing more faithfully all the objects nature within the FoV under analysis.

The filter that spans this multitarget problem follows similarly the procedure found in single target filters: initialization, prediction, correction and state estimation. The proof of this approach, given in [12],[4],[16] and papers such as [6],[5], are left as theoretical reference because they form the academical background and support of this thesis but do not include further information to the understanding of this work. The commented procedure steps can be described as it follows:

- Initialization: The little knowledge about the surroundings of the AD vehicle points toward the use of a process already studied before: the Poisson Process, with high spatial state uncertainty or variance of targets in the FoV. Everything is uncertain to some level, which suits faithfully the reality around the ADAS.

- Prediction: Having in mind the set integral calculation and evaluation technique[15], the prediction step can be resolved as follows

$$f_{k+1|k}(\mathcal{X}|\mathcal{Z}^{(k)}) = \int f_{k+1|k}(\mathcal{X}|\mathcal{X}') \cdot f_{k|k}(\mathcal{X}'|\mathcal{Z}^{(k)})\, \delta\mathcal{X}'. \tag{3.40}$$

- Correction: Similar to the single target corrector, the Bayesian approach for the multitarget filter becomes

$$f_{k+1|k+1}(\mathcal{X}|\mathcal{Z}^{(k+1)}) = \frac{f_{k+1}(\mathcal{Z}_{k+1}|\mathcal{X}) \cdot f_{k+1|k}(\mathcal{X}|\mathcal{Z}^{(k)})}{f_{k+1}(\mathcal{Z}_{k+1}|\mathcal{Z}^{(k)})} \text{ where} \tag{3.41}$$

$$f_{k+1}(\mathcal{Z}_{k+1}|\mathcal{Z}^{(k)}) = \int f_{k+1}(\mathcal{Z}_{k+1}|\mathcal{X}) \cdot f_{k+1|k}(\mathcal{X}|\mathcal{Z}^{(k)})\, \delta\mathcal{X}. \tag{3.42}$$

[15]Refer to math handbooks or [12] for multiple objects mathematical analysis.

- State estimation: As [12] explains clearly, the multiple target state estimators like Maximum a Posteriori (MAP) and Expected A Posteriori (EAP) become inappropriate. Additionally, it revisits the Marginal Multitarget (MaM) and Joint Multitarget (JoM) estimators and resolves the calculation cost throughout the Gaussian Mixture approximation.

3.5.1 The Detected Multitarget Density

The Bernoulli Process is a RFS process that describes any finite, independent and identically distributed random set Bernoulli distributed, $\mathbf{\Psi}_k^B$ [6]. Note that the nature of the process points to a single element set with probability of existence r and space state distribution f; being the $\mathcal{GGIW}$ the single extended target f spatial distribution with probability of existence $r \in [0, 1]$. Then, the probability distribution of any element that is part of this set will be described by

$$f(\mathcal{X}) = \begin{cases} 1 - r, & \mathcal{X} = \emptyset \\ r f(\mathbf{x}), & \mathcal{X} = \{\mathbf{x}\} \rightarrow |\mathcal{X}| = 1 \\ 0, & |\mathcal{X}| \geq 2. \end{cases} \tag{3.43}$$

Moreover, extending the idea that targets are assumed to be independent and Bernoulli distributed, one can directly describe[16] the FoV as a Multi-Bernoulli environment with the following random set and probability density function

$$\boldsymbol{\mathcal{X}} = \biguplus_{i \in \mathbb{I}} \mathcal{X}^i \text{ and} \tag{3.44}$$

$$\tag{3.45}$$

$$f(\boldsymbol{\mathcal{X}}) = \begin{cases} \sum\limits_{\uplus_{i \in \mathbb{I}} \mathcal{X}^i} \prod\limits_{i \in \mathbb{I}} f^i(\mathcal{X}^i), & |\boldsymbol{\mathcal{X}}| \leq |\mathbb{I}| \\ \\ 0, & \text{otherwise} \end{cases} \tag{3.46}$$

3.5.2 Global Hypotheses Tracking: The Mixture

One of the main characteristic of the Poisson Multi-Bernoulli Mixture filter is that it is based on hypotheses tracking, this is, each of the Multi-Bernoulli might turn into new Multi-Bernoulli distributed spaces each k-time step. This exponential increase is due to combinatorial possibilities, also known as data associations.

[16] Note that the multitarget distribution is based on the existence of the object, thus the object must have been detected in order to apply eq. 3.46.

Different hypotheses must be examined and input to the forthcoming time steps to conclude in the most likely scenarios[17] which is done by weighing each track using its corresponding likelihood[18].

The likelihood ratios assigned to each of the tracks do not represent still a global hypotheses, but, they can be obtained by normalizing all the tracks likelihoods at a certain k-time step. Once this mixture, normalization step, is done, one could select the most probable global hypotheses and the corresponding track. This scalar describing the mixture is called weight, $\mathcal{W}$, and is indexed by $j \in \mathbb{J} \,|\, j = [1, |\mathbb{J}|]$; leading to the $\mathcal{W}^j$ for each track global likelihood[19].

3.5.3 The Poisson Multi-Bernoulli Mixture Density

Up until now, the two main RFS processes behind the PMBM filter have been studied: the Poisson Point and the Multi-Bernoulli Mixture processes of which expressions are found in previous sections.

Now, the last step to take towards the Poisson Multi-Bernoulli Mixture filter is the union of these two kinds of RFS, describing all possible objects inside the FoV. This is done by applying again independence between undetected and detected objects as

$$\boldsymbol{\mathcal{V}} = \boldsymbol{\mathcal{X}}^d \biguplus \boldsymbol{\mathcal{X}}^u, \tag{3.47}$$

and this derives into the final density of

$$f(\boldsymbol{\mathcal{V}}) = \sum_{\boldsymbol{\mathcal{X}}^d \biguplus \boldsymbol{\mathcal{X}}^u} f^u(\boldsymbol{\mathcal{X}}^u) \sum_{j \in \mathbb{J}} \mathcal{W}^j f^j(\boldsymbol{\mathcal{X}}^d) \text{ where} \tag{3.48}$$

$$\text{PPP process is } f^u(\boldsymbol{\mathcal{X}}^u) = e^{-\langle D^u;1\rangle} \prod_{\mathbf{x} \in \boldsymbol{\mathcal{X}}^u} D^u(\mathbf{x}) \text{ and} \tag{3.49}$$

$$\text{MBM process is } f^j(\boldsymbol{\mathcal{X}}^d) = \sum_{\uplus_{i \in \mathbb{I}^j} \mathcal{X}^i = \boldsymbol{\mathcal{X}}^d} \prod_{i \in \mathbb{I}^j} f^{j,i}(\mathcal{X}^i). \tag{3.50}$$

Employing everything studied until now and remembering the fact that the single target model density is parameterized by the conjugate prior of the $\mathcal{GGIW}$,

[17] It is highly important to keep more than the most likely scenario or MB.

[18] The procedure involves taking the product of the analyzed $\ell_{\mathcal{GGIW}}$ likelihood of each target.

[19] Please note once again that the nature of MHC tracker requires holding more than one MB. A complete different aspect is to select the most likely one from the *actual group of MBs* and work with it *temporary*, just under the current or analyzing k-time step.

the PMBM density presented previously, eq. 3.48, gets fully described at both correction and prediction stages and at a certain k-time step by

$$D^u; \{\mathcal{W}^j, \{(r^{j,i}, f^{j,i})\}_{i\in\mathbb{I}^j}\}_{j\in\mathbb{J}}. \tag{3.51}$$

The algorithm or pseudo-code to process these filter parameters, eq. 3.51, can be found in [6]. In what it follows, the stochastic optimization (SO) applied to Radar data is introduced, which is fundamental when it comes to associate the acquired data with a source within the FoV.

3.6 Data Association with Stochastic Optimization

The unknown origin of the measurements leads to different possible DA between any source or target and the measurement(s). All these measurements are grouped in the previously mentioned $\mathcal{Z}$ set, without any tag or label describing the location of the targets. Notice that each target can be the source for different measurements, whereas one particular measurement can not come from different sources.

A term called Cell, C, is introduced, since it will be central aspect of the DA. Recall from previous sections that there are two different sets of indexes, $\mathbb{I}$ and $\mathbb{M}$. The filter correction/update step that is committed to reduce the uncertainty derived from the prediction is fed with these associations between possible targets and measurement(s). They group cells and contain explicitly and implicitly target indexes from the target-index set, $i \in \mathbb{I}$, and measurement(s) index from the $m \in \mathbb{M}$ index set, respectively.

For instance, if the sets are composed by $\mathbb{I} = \{i_1, i_2\}$ and $\mathbb{M} = \{m_1, m_2, m_3, m_4\}$, possible cells can be described as:

$$\begin{aligned} C_1 &= \{i_1, m_1, m_2\} \\ C_2 &= \{i_2\} \\ C_3 &= \{m_3, m_4\} \end{aligned}$$

These three cells, $(C_c \,|\, c = 1, ..., |A| = 3)$, describe one possibility of combining the existing data, where C_1 associates i_1 and measurements $\mathcal{Z}_{C_1} = \{\mathbf{z}_{m_1}, \mathbf{z}_{m_2}\}$ together;

C_2 does not hold any measurement, $\mathcal{Z}_{C_2} = \{\emptyset\}$, and C_3 does not associate any of the existing targets to the group of $\mathcal{Z}_{C_3} = \{\mathbf{z}_{m_3}, \mathbf{z}_{m_4}\}$, meaning that there is a new object, i_3, within the FoV.

The previous A stands for the association space that is formed with a possible combination that has been observed, for example, $A = \{C_1, C_2, C_3\}$. Any A association space is a subset of the entire j^{th} global hypothesis association hyperspace, $A \subset \mathcal{A}^j$ [20]. These combinations can be obtained after running any DA algorithm, for instance, the a stochastic optimized algorithm.

The associations can have different lengths, what it might be of disadvantage if computationally efficient codes are needed. One approach to solve the burden imposed by the different cell sizes is using the Assignment Vector, φ or AV. It is of fixed length, $|\mathcal{Z}| = |\mathbb{M}| = M$, and it represents a descriptive array where the association between any target and measurement(s) is described by a φ_m parameter. In conclusion, the AV is a compact way to associate targets and measurements of $A \subset \mathcal{A}^j$, through a fixed $|\mathcal{Z}|$-length array.

Revisiting the previous cells example, the representation of the Assignment Vector (AV) can be expressed then as $\varphi = [\varphi_1, \varphi_2, \varphi_3, \varphi_4] = [1, 1, 3, 3]$, each φ_m being an association between a specific measurement and an exact target.

The approach used for DA, found in [7] and claimed to outperform C&A methods and Monte-Carlo Markov Chain (MCMC) sampling methods[21], is basically based on taking random steps following the actions, called α-actions,

- *Do Nothing*: The initial Assignment Vector that is to be processed is not changed, this is, the target indexes assigned to each of the assignment vector elements remain similar to the previous time step:

$$\varphi_{\mathtt{SO}}^{\alpha_1} = \varphi^{\text{Initial}}$$

- *Gibbs sampling*: Provided that a random integer, $r_1 \in \{1, ..., |\mathtt{AV}|\}$ that can point to any $\varphi_{m=r_1}$, the target index inside φ_{r_1} is extracted firstly and the $\mathbf{z}_{m=r_1}$ measurement is then assigned to other existing target indexes. The

[20] One possible combination, A, of all possible spaces of j^{th} global hypothesis, $\mathcal{A}^j$.
[21] C&A are two steps method that perform firstly clustering and assignment then.

action ends with all possible allocations of the measurement into other cells than $C_{\varphi^{\text{Initial}}_{m=r1}}$:

$$\varphi^{\alpha_2}_{\texttt{SO}} : \boldsymbol{\varphi} \leftarrow \forall \varphi^{\text{Initial}}_m \mid \varphi_m \in \mathbb{I} - \{\varphi_{r1}\}$$

- *New Cell*: The previous actions are derived by moving a particular measurement from its initial target index, φ_{r_1}, to any other existing indexes in $i \in \mathbb{I} \mid i \neq i_{r_1}$. Now, there is always the chance that a new target has entered the FoV and this target must be tagged or labelled with a new target index, such as $i_{\text{New}} \mid \mathbb{I}^{k+1} = \mathbb{I}^k \cup i_{\text{New}}$. Hence, the action to take is to move the commented measurement that is saved in $\mathbf{z}_{r_1}$ to a new cell:

$$\varphi^{\alpha_3}_{\texttt{SO}} : \varphi \leftarrow \varphi^{\text{Initial}}_m \mid \varphi_{m=r_1} \notin \mathbb{I}^k$$

- *Split*: For previous actions, only one random index was sampled from a set of length $|\varphi^{\text{Initial}}|$. For the following splitting action another random index is introduced, r_2, which will enable to group the initial assignment into two new assignments. The procedure two group is suggested to be the *k means*$_{++}$ algorithm [7]; refer also to [8], [7], [6] and [1] for information about the commented theory. However, in the simulation step of this project, a bottleneck was found in the split with the *K-means++* approach; thus a similar procedure was implemented with same results.

The related pseudo code is

$\texttt{v}_{\texttt{idx}} = [p_1, ..., p_j, ..., p_{|\texttt{f}|}] \mid p_j \in \{1, 2\}$ and $\texttt{f} = \texttt{find}(\texttt{AV}^{\text{Initial}}(\texttt{r1}) == \texttt{AV}^{\texttt{Initial}}(\texttt{r2}))$.

Note here that the split is conditioned on both p_i and $\texttt{f}$, being $\texttt{f}$ a vector with assignment indexes containing the same target indexes. In addition, the cell under analysis can be assigned to either an existing one or to a new one, denoted as α_{4_1} or α_{4_2}. The obtained AV after SO:

$$\begin{aligned}\varphi^{\alpha_{4_1}}_{\texttt{SO}} = (p_j == 1) * [\varphi^{\text{Initial}}_{\texttt{f(v}_{\texttt{idx}}\texttt{==1)}} \leftarrow \forall i \in \mathbb{I}^k - \{i_{r1}\}] \quad + \\ (p_j == 2) * [\varphi^{\text{Initial}}_{\texttt{f(v}_{\texttt{idx}}\texttt{==2)}} \leftarrow \forall i \in \mathbb{I}^k - \{i_{r1}\}]\end{aligned}$$

$$\begin{aligned}\varphi^{\alpha_{4_2}}_{\texttt{SO}} = (p_j == 1) * [\varphi^{\text{Initial}}_{\texttt{f(v}_{\texttt{idx}}\texttt{==1)}} \leftarrow i \notin \mathbb{I}^k] \quad + \\ (p_j == 2) * [\varphi^{\text{Initial}}_{\texttt{f(v}_{\texttt{idx}}\texttt{==2)}} \leftarrow i \notin \mathbb{I}^k]\end{aligned}$$

- *Merge*: Instead, if $\varphi_{r_1} \neq \varphi_{r_2}$, then the cells are candidates to merge. In this case, there is only one way of assignment:

$$\varphi_{\mathtt{SO}}^{\alpha_5} = \forall \varphi^{\text{Initial}}_{(\varphi_m^{\text{Initial}} == i_1)} \leftarrow \varphi_{r2}^{\text{Initial}}$$

It is commented in the same paper, which it is also applied to the scope of this project, that the method does not hold Markov Chain properties (due to the non possibility to return back to the previous step), making it inappropriate to sample from. However, the aim is to associate the measurements with the targets and not to sample from a distribution. The implementation aspects can be found in the paper [8].

DA decision-making step: In each iteration t, one assignment $\varphi^{(t)}$ is obtained. Notice that the five α-actions must be iterated several times, $t \in \mathcal{T} = \{1, ..., |A^j|\}$ (as it can be seen in [6] and [8]), to ensure all the assignment indexes from AV are crossed enough times.

After some manipulations and deductions, the decision-making factor, associated to each of the iterated α-action, results in the following probability[22]:

$$P\{\varphi^{(t+1)} = \varphi_\alpha^{(t)} | \varphi^{(t)}\} = \frac{\mathcal{L}_\alpha^{(t)}}{\sum_{\alpha'} \mathcal{L}_{\alpha'}^{(t)}} \tag{3.52}$$

This eq.3.52 or likelihood ratio will enable to select the $A \subset \mathcal{A}^j$ or most likely AV spaces, contributing to the proper correction or update of the prediction step.

[22]The $\mathcal{L}$ likelihoods are resolved by taking the product of each of the $\ell_{\mathcal{GGIW}}$ of each target or object within the FoV.

Chapter 4

Methodology

The validation of the previously commented theory should be carried out throughout specific evaluation methods that allow to express the results feasibly. Furthermore, the simulated results will be valid *only if* there exists a ground truth scenario which can be compared to. One should recall that the ground truth is a term which contains the necessary and trustworthy information by which new algorithms can be tested and validated.

Therefore, the following sections are devoted to introduce both the employed coding language and the metrics introduced.

4.1 Programming Language

This project has been implemented in MATLAB, which comes convenient when mathematical environments are to be tested. Moreover, in order to represent the tracking scenario as realistically as possible, oo-programming (object oriented programming) has been employed. The reason behind the use of the oo-programming lays on the fact that these objects, dynamical in their properties during process time, reproduce closely the real situations. Moreover, the application of this kind of coding is thought to result in such superior performance, in case some assumptions about the objects such as the `handle` class are taken.

An oo-program exploits the idea of classes that are meaningful in this particular project, the description of *targets* with *objects*[1]. It also comes handy when the representation of the attributes or properties, held within each target, are to be

[1]Since the nomenclature might come confusing when objects from oo-programming and the objects from the FoV are to differ, the use of target nomenclature or name instead of objects has been thought to be applied in this section.

parameterized. The reader should now recall the section Modelling, in which the $\mathcal{GGIW}$ single extended target modelling was introduced. Notice that the mentioned model is built upon a set of 6 parameters, ζ, that are the only and necessary descriptors to represent the density function of conjugate prior nature. Note also that since the Multi-Bernoulli process is used, the targets are assumed to be *independent* and *identically* distributed over the FoV.

In what follows, brief explanations about the steps taken and the reasoning behind are outlined. It is thought that further explanations about the chosen steps would not make any point, since the main aim at which this thesis is targeted is the transmission of the idea of PMBM filter performance, with valid/trustworthy results and not how it is coded or written down.

Firstly, the previously commented two kinds of objects are introduced, which are important when it comes to describe any of the needed parameters. Then, different levels inside these commented classes are presented, as well as, the meaning of them in the PMBM algorithm.

So, let's first explain an important condition that changes the nature of a class and by derivation the nature of each of the targets. This particularity is the heritage obtained by the commented super-class `handle`. Assume two kind of classes: `value` class and `handle` class[2]. If the class is inheriting the super-class `handle`, then the objects represented by this class will not store previous information; thus containing just at-the-moment properties values. The use of only certain data (discarding previously obtained one) enhances the performance of the code and describes the targets dynamical natures. Therefore, it is of such sensible approach to use the `handle` super-class as a way to describe every target within the FoV. The following scheme was coded to be the appropriate representation of the analyzed targets.

[2]Please note that the employed language is MATLAB, and thus the way the class is known might change from language to language.

- FoV$_k$ [project]
  - Prediction/Correction Target Object Space [funcs]
    - Su(Nu): Undetected Targets Disjoint Union [struct.class < value]
      - ggiw: ζ_u [class < handle]
        - alpha [scalar]: α_u
        - beta [scalar]: β_u
        - m [vector]: $\mathbf{m}_u$
        - P [matrix]: P_u
        - v [scalar]: v_u
        - V [matrix]: V_u
      - w: weight [scalar]
    - Sb(Nb): Birth Targets Disjoint Union [struct.class < value]
      - ggiw: ζ_b [class < handle]
        - alpha [scalar]: α_b
        - beta [scalar]: β_b
        - m [vector]: $\mathbf{m}_b$
        - P [matrix]: P_b
        - v [scalar]: v_b
        - V [matrix]: V_b
      - w: weight [scalar]
    - Sf(Nf): Detected Targets Disjoint Union [struct.class < value]
      - ggiw: ζ_d [class < handle]
        - alpha [scalar]: α_d
        - beta [scalar]: β_d
        - m [vector]: $\mathbf{m}_d$
        - P [matrix]: P_d
        - v [scalar]: v_d
        - V [matrix]: V_d
      - w: weight [scalar]
    - W(j): Global Hypotheses Weights [vector]
    - A(j): j^{th} Assignment Vectors [vector/matrix]

This shown "super"-object space is one of the possibilities that the abstract representation of all variables and parameters within the FoV might take. Note that this is all the necessary information required to depict all possible targets that appear within the sensors view area. Recalling the argument explained about synthesis, the pseudo-code or flow-chart employed in the code can be found in the Appendix A: Pseudo-code/Flow-chart.

4.2 Metrology

Cited directly from [12], this discipline refers to "[...] the process of determining the degree of similarity or dissimilarity of entities of interest. It is central to information fusion, whether we are to compare competing algorithms with each other or, within an algorithm, to determine the influence of internal parameters on the algorithm's performance.". In other words, it is a fundamental field when it comes to provide solid results and trustworthy comparisons between available algorithms.

As it is also explained in [12], the same procedure applied to the single target metrology can be applied to the multitarget metrology, which it is based on metrics or distance functions. A reliable distance function must satisfy several conditions called distance axioms, explained in [2], and it is usually described by either the difference between two points in a fixed set [10] [12], such as *Euclidean distance*, or distances between two probability distributions [12], such as *Kullback-Leibler distance*.

The reader should have noticed and recalled that the targets are not anymore represented by points, but by cloud-points; hence, the commented two distances turn into distributions. The resulting metrics are: *Wasserstein Distance WD* and *General Optimal Subpattern Assignment GOSPA*.

4.2.1 Gaussian Wasserstein Distance

It becomes natural to this mathematical subject that when a topology of a set is presented, a way to measure distances[3] between the elements inside the set is included. The use of different extents, but the Random Matrix one, makes the derivation of this metric sometimes impossible to express in closed-form [20]. However, due to the Random Matrix formulation applied throughout the project, precisely to the description of the extent, enabled a closed-form expression, known as the *Gaussian Wasserstein Distance* [20] [12] [2].

The *Wasserstein Distance* can be expressed as

[3]Distance could be also thought as similarities in their nature, and how different they are from each other. For instance, the distance between two distributions is carried but comparing how similar these distributions are.

$$d(\mathcal{X}, \hat{\mathcal{X}}) = \min_{\pi} \sqrt{\frac{1}{n} \sum_{i=1}^{n} \|\mathbf{x}_i - \hat{\mathbf{x}}_{\pi i}\|^2}, \tag{4.1}$$

where π and $\hat{\mathbf{x}}$ represent permutation and estimate of the state at i permutation, respectively. Assuming an ellipse extent such as the Random Matrix, it derives into

$$d_{\mathrm{G}}(\mathcal{N}_{\mathbf{x}}, \mathcal{N}_{\hat{\mathbf{x}}})^2 = \|m_{\mathbf{x}} - m_{\hat{\mathbf{x}}}\|^2 \quad + \quad \mathrm{Tr}\left(\Sigma_{\mathbf{x}} + \Sigma_{\hat{\mathbf{x}}} - 2\sqrt{\sqrt{\Sigma_{\mathbf{x}}}\Sigma_{\hat{\mathbf{x}}}\sqrt{\Sigma_{\mathbf{x}}}}\right). \tag{4.2}$$

Where Σ stands for the covariance of any Gaussian distribution. Notice how the extension gets parameterized by the the mean and covariance values as: $\mathcal{N}(\mathbf{m}, s\Sigma)$ where s behaves as a scaling factor. From eq.4.2 and [20], one could say that this particular metric is sensitive to the distance between two centers or mean values, m_x and $m_{\hat{x}}$; being the mean a substantial factor of this metric.

Therefore, if the target with its position and extension is similar to its estimate, the Gaussian Wasserstein distance will tend to zero. Intuitively, this reflects that the estimate, $\hat{\mathbf{x}}$, will be close to the real target state *if and only if* the *Gaussian Wasserstein Distance* tends to a stable value. Therefore, it is obvious that this stable value is the limit for the assessment of real single target and estimate states.

Both [15] and [12] compare different target scenarios and different metrics or distances such as *Hausdorff Distance*, *Wasserstein Distance* or *OSPA*; concluding differently when it comes to choose among these metrics. For instance, it comments that *Hausdorff* is not appropriate to the problem of multitarget tracking metrics since it is not sensitive to the differentiation of the cardinality of a finite set, which should be core to this project. As for the downsides of *Wasserstein Distance*, some are: the metric is inconsistent in the sense of balancing the locations of the estimates around the real state, see given example and figure [15, p. 3]; the metric and its theoretical base are not trivial to follow; it can be not adequate for the multitarget filtering due to the loss of the distance axioms[4]; etc. In case the reader needed complementary information to this thesis, she/he could refer to the commented [15] or [12].

[4]After the transformations suffered in case of multitarget scenarios; going from single to multiple targets metric.

Previously commented, a solution to the aforementioned situation is the employment of the *GOSPA*, based on *OSPA*, and standing for (General) Optimal Subpattern Assignment. It addresses some of the problems that the *OSPA* metric has when Point Process Theory is used and it can be found in the literature in different papers and books; which in the case of this thesis is [14].

4.2.2 General Optimal Subpattern Assignment (GOSPA)

The convenience that *OSPA* offers when it comes to compare mathematically a finite set is not applied to the assessment of a multitarget scenario. Precisely, in the *OSPA* metric, the importance of the error in the position of any particular target existing in the FoV is not of relevance, this is, the type of the object is not taken into account to calculate the error/distance.

However, *GOSPA* is the transformation derived from *OSPA* that enriches the already commented algorithm penalizing the location errors of different types of targets within the FoV as

$$d_p^{c,\alpha}(\mathcal{X},\mathcal{Y}) \triangleq \left(\min_{\pi \in \prod_{|\mathcal{Y}|}} \sum_{i=1}^{|\mathcal{X}|} d^{(c)}(\mathbf{x}_i, \mathbf{y}_{\pi(i)})^p + \frac{c^p}{\alpha}(|\mathcal{Y}| - |\mathcal{X}|) \right)^{\frac{1}{p}}. \quad (4.3)$$

where π, c, α and p stand for permutation, maximum allowable localization error, normalization factor and number of penalized outliers, respectively [14] [15].

Several properties can be derived from [14] such as how to tune the α parameter and how costly, in terms of $\frac{c^p}{\alpha}$, it will be if the real and estimate states are far apart. One deduction from the cited paper that one should extract is the tuning as $\alpha = 2$; meaning that the cost of being missed target or false target will be the same, independent from how it is assigned throughout the permutations. It is stated that selecting $\alpha = 1$, the distance results in an "unnormalized" *OSPA* that is not proved to be a metric.

It becomes a logical choice to opt for the tuned ($\alpha = 2$) *GOSPA*; in order to represent the surroundings of an ego-vehicle, since the FoV might be clustered by different kind of targets that are not only the detected ones.

4.3 Approximations

It is of high importance and for the sake of efficiency to approximate the PMBM algorithm up to some extent. Note that if proper selections of the approximations are applied over the parameters that constitute the filter, it might result in having a better performance under permissible trade-off:s.

The approximations applied in this particular thesis can be split in three groups: the ones taken by the author [6]; the ones related to the project and the ones that are derived from the coding process of the PMBM filter. Since the ones taken by the author already represent the same filter composition, it was thought that they are only worth commenting; leaving the reader with [6], [7] and the remaining literature for further explanations. Thus, the approximation can be listed as:

- *Part of the filter*: As it was explained, the filter is applied upon a dense scenario which is composed by different kinds and number of targets. Moreover, the procedure of analyzing "every target[5] with every measurement" is of high-computational cost; leading to inefficiency.

  This association increase can be mitigated by two different approximations, also presented in [7], which are: likelihood based weights and relative frequency based weights approximations. They are based on calculating likelihoods ratio and sampling from a stable distribution[6], respectively. The one selected for the aim of this project is the likelihood based weights approximation, assigning the weights linked to a random subset associations space by the use the commented likelihoods ratio. Please refer to the cited paper for further information about the approximation methods.

- *Assumptions taken that are not imposed by the user*: These assumptions can be found, for instance, in [6]. Among these approximations one can find the treatment and values assigned to the p_D, p_S and p_{Death} for each of the targets. The project has been designed to have the next probabilities assigned similarly for every target as $p_S \approx 0.98$ and $p_D \approx 0.98$ values; motivated by the idea that everything within the FoV should be likely to survive and detect when it comes to the evaluation of the PMBM filter. Due to these high probabilities, the probability of death or pruning of the targets of the FoV, dependent on the probability of existence, was thought to be set high enough, $p_{\text{Death}} \approx [0.6, 0.8]$.

[5]Here *every* not only gathers the number of objects, but also the type of them.

[6]Therefore, a period for stabilization of the distribution is needed, which is obtained by running more samples.

Parameters such as scanning volume A, α and β were thought to be scaled approximately to the extension of the ego-vehicle, this is, to the assumption that the vehicle would have $\frac{l}{w} \approx 2$ size- or shape-relation.

- *Approximations employed on MATLAB*: They were taken due to the necessity of coherence and efficiency of all the objects found throughout the scripts[7]. For example, important assumptions were made in the way undetected targets are treated. If one refers to the prediction intensity of undetected targets, as well as, PPP update missed detection, one would obtain[8]:

$$\begin{aligned} D_{+}^{u}(\mathbf{x}) &= \sum_{n=1}^{N^b} w^{b,n}\mathcal{GGIW}(\mathbf{x};\zeta^{b,n}) \\ &\quad + \sum_{n=1}^{N^u} w^{u,n} p_S(\hat{\mathbf{x}}^{u,n})\mathcal{GGIW}(\mathbf{x};\zeta_{+}^{u,n}) \\ D^{u}(\mathbf{x}) &= \sum_{n=1}^{N^u} (w_1^{u,n}\mathcal{GGIW}(\mathbf{x};\zeta_1^{u,n}) + w_2^{u,n}\mathcal{GGIW}(\mathbf{x};\zeta_2^{u,n})) \end{aligned}$$

Owing to the necessity of saving both birth and undetected parameters into a single undetected variable, as well as, both w_1 and w_2 weigths in the update/correction step, the following decisions were applied:

$$\mathtt{Threshold_t} = 0.4 \tag{4.4}$$

$$\mathtt{Su_{k-1}(nu).w} < \mathtt{Threshold_t} \rightarrow \mathtt{prune(Su_{k-1}(nu_{w<t}))} \tag{4.5}$$

$$\mathtt{Su_k^{+}} = [(\mathtt{Su_{k-1}^{pruned}})^{+}, \mathtt{Sb}] \tag{4.6}$$

$$\mathtt{w_1} > \mathtt{w_2} \rightarrow \mathtt{select}\,(\mathtt{w_1};\zeta_1) \quad \mathtt{otherwise} \quad \mathtt{select}(\mathtt{w_2};\zeta_2) \tag{4.7}$$

The expressions for both $(\mathtt{w_1};\zeta_1)$ and $(\mathtt{w_2};\zeta_2)$ can be found in [6]. The motivation to select the values the way presented is based on thresholding and comparison. The basic idea of the previous approach is focused on the importance of the weights in the D intensity; where the smart use of them provides a more efficient computation.

4.4 Initialization

This following section is intended to explain the initialization stage and the values that might be introduced to each of the filter procedures. Two kinds of initialization have been classified: the ones belonging to prior knowledge needed in every

[7]Note once again that *object*, in this particular bullet point, refers to the way oo-programming is thought to be understood and do not directly refer to the targets of the FoV.

[8]Recall that the use of conjugate prior enables the parameter-characterization of the filter.

Markov chain initial state to combat sensitiveness and the specific initial information required in the SO algorithm to increase efficiency.

The filter has to be initialized so that it can start working with some parameters even if they are uncertain. This initialization is part of the birth settings and depending on the conditions of the environments and the vehicle setup, different starting conditions can be implemented. The tuning will be shown in the Results section and it will be possible to see how changing it slightly affects considerably the tracking of the vehicles.

4.4.1 Prior Sequence Knowledge

There must be always knowledge of some kind even if it is uncertain and does not represent truly the surroundings of the AD vehicle. In other words, the necessity of an uncertain prior state representing initial $[t_0] = 0$ time step is imperative, since the forthcoming state is *always* based in the previous one.

In what it follows, the how-to-set some of the filter prior parameters such as $\mathcal{GGIW}$ are shown.

- V **(FoV volume) and** d **dimension for** $\mathbb{R}^d$: Since the FoV is highly dependant on the sensors resolution and capabilities, the volume the scanning might take was assumed to be of the order of $200\,\mathrm{m}^3 = 10\mathrm{m} \times 2\mathrm{m} \times 10\mathrm{m}$. The project was also assumed to be on XY-plane, since height was not an interesting parameter motivated by the employment of the filer in urban scenarios. Therefore, $d \to \mathbb{R}^2$ [9].

- **Measurement Rate**: The Poisson distribution is again used to described the amount of measurements that one might find assigned to targets. After some rehearsals, it was concluded that the measurement rate, governed by the Poisson rate, should be around $\lambda = \{3, 4\}$. This will allow to assume targets with 0 to around 10 measurements assigned; representing the true amount of measurements associated to each target.

- α **and** β **parameters**: From the Gamma distribution theory, the following moments can be obtained: $\mathbb{E}[\gamma] = \frac{\alpha}{\beta}$ and $Var(\gamma) = \frac{\alpha}{\beta^2}$ where $\gamma \in \Gamma$. If the measurements are thought to be distributed as explained previously, one could obtain then $\alpha = 4\beta$ and $\alpha = 2\beta^2 \to \beta = \{0, 2\} \to \alpha = 8$; where $\beta = 0$ is not a valid option.

[9] Assuming no elevation.

- q **process noise**: The process noise is understood and formulated as follows:

$$Q = G_{Q_{\text{CV}}} * q * 1_{2\times 2} * G_{Q_{\text{CV}}}^T \text{ where } G_{Q_{\text{CV}}} = \begin{bmatrix} \frac{T_s^2}{2} \times 1_{2x2} \\ T_s \times 1_{2x2} \end{bmatrix}$$

  The q is assumed to be the standard variation, thus $q_{\text{Var}} = q_{\text{Dev}}^2$. Different values have been used, taking different meanings depending on the situation; but the values have been assumed to span $0.001 < q \leq 1$. They were thought to represent straight motions, rather than randomly rotating motions.

- M **rotation matrix**: Explained before, sometimes it is necessary to introduce rotational behaviours into the motion models, and thus there is also the need to track these rotations. This characteristic is known as rotation matrix, $M_{XY} = \begin{pmatrix} \cos\theta & -\sin\theta \\ \sin\theta & \cos\theta \end{pmatrix}$, which gathers the orientation changes through trigonometry and $\theta = \Delta\phi$ heading. Now, one of the approximations or assumptions made was to deduce that all the motions can be described with the CV model. It results that in this particular case the rotation ends in the identity matrix of dimension $d = 2$, since the heading does not change from time step to time step, $\phi_k = \phi_{k+1}$.

- **Extent**: Two parameters can be found describing the extension: the degrees of freedom, v, and the Random Matrix V of the Inverse Wishart distribution. If one checks the equations related to the $\mathcal{GGIW}$ single target procedure, she/he will see that degrees of freedom are fundamental for the estimate of the extension, and they have to be high enough to make possible the characterization of it. The greater the degrees, the better would be estimate the extension. For instance, throughout the project the initial value assigned to the degrees of freedom is between $15 < v < 25$, considering that the highest possible amount of measurement, related to a single target, stays around 8 to 10^{10}.

  As it has been shown before, the initial Random Matrix value was thought to be of width 2 and length 4 in metres. This might not be representative of all the objects and all scenarios (as it will be seen afterwards), thus it is not the most efficient initialization. Even so, since the estimate will, at some time step, converge with the reality, the proposed initialization was left as standard to almost all kind of targets.

- τ **and** η **parameters**: The presented parameters can be understood as similar to the process noise but related to the extension uncertainty. Exact values are given in the appendix section.

[10] Please check the Measurement Rate point for this statement.

4.4.2 DA initialization

The DA algorithm is in charged of obtaining associations derived from several actions and assigning corresponding likelihood weights to each of the Assignment Vector.

There exists the possibility to initialize it, refer to [7], in order to reduce computational time, provided that an initial Assignment Vector is given. The procedure for this is based on likelihood calculations, as the SO, but instead of making associations and weighting them, the measurements are run individually and weighted accordingly as

$$\varphi_m^{(0)} = \begin{cases} \hat{i}_m & \text{if } \hat{i}_m \in \mathbb{I} \\ m + |\mathbb{I}| & \text{otherwise} \end{cases}, \tag{4.8}$$

$$\hat{i}_m = \arg\max_{i \in \mathbb{I} \cup \{0\}} \ell_{j,i}^{m,\text{Init}}, \tag{4.9}$$

$$\ell_{j,0}^{m,\text{Init}} = \lambda c(\mathbf{z}^m) + p_D \langle D^u; \ell_{\{\mathbf{z}^m\}} \rangle \text{ and} \tag{4.10}$$

$$\ell_{j,i}^{m,\text{Init}} = p_D r^{j,i} \gamma(\hat{\mathbf{x}}^{j,i}) \phi(\mathbf{z}^m \mid \hat{\mathbf{x}}^{j,i}). \tag{4.11}$$

This simple idea will allow to reduce, as shown in Results section, the necessary time the SO algorithm needs to process.

Chapter 5

Results

This section gathers the assessment of the theoretical concepts described before, from the visualization of what the theory says to the evaluation of the PMBM filter as a method to track dense scenarios like the urban landscape. Furthermore, since one of the final aims might be the implementation of this filter into a real vehicle system, archicture or code profiles with the elapsed times are also given.

The employed methods are validated upon two environments: the simulation environment, where synthetic data is created and tested with the metrics explained before[1], and the real scenario, provided by the SafeRadar Research company. In this last case, the ground truth is not available through any other kind of source, such as a photographic one, but the environment where the data was acquired is known.

Since one of the aims of the project is to test the Poisson Multi-Bernoulli Mixture filter with different kinds of data environments, different figures were obtained and examined. The figures are not necessary but they help to understand the project and can be found in Appendix B: Complementary figures for evaluation.

[1]Each of the scenarios, this is, both single extended target and multiple extended targets.

5.1 Simulated Environments

5.1.1 Single Extended Target Model - $\mathcal{GGIW}$

Since the multiple extended targets scenarios are formed by the single extended target, an analysis of this is introduced in this section.

Before evaluating the $\mathcal{GGIW}$ model, the following figure was thought to be given, to show how the $\mathcal{GGIW}$ looks and what to expect from the multiple targets filtering. Remember that the measurements likelihood are normally distributed, with the extension being the covariance of the distribution under analysis. This can be seen in fig. 5.1.1, where measurements points fall within/on/out the extension. These different positions follow the σ-levels describing the different covariances of an ellipse. In case the reader wants to see it, please go to Appendix B and check these levels and measurements relations for one time step object.

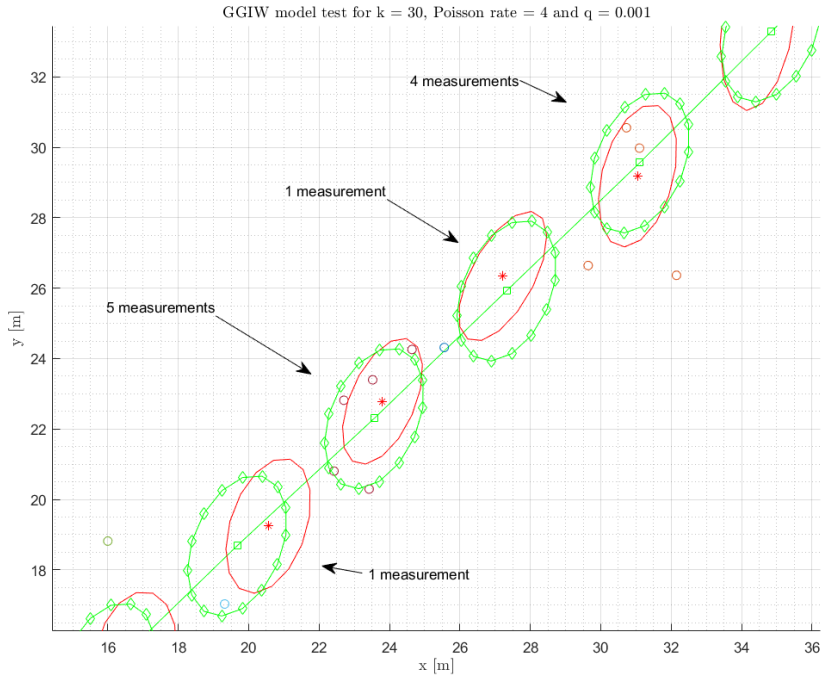

Figure 5.1.1: A snippet of the $\mathcal{GGIW}$ performance.

In red, the estimated extensions are shown, while in green the real target extension is displayed. Note that from time step to time step the measurement amount

changes, due to dependency on Poisson distribution. It gets visible, from the fig. 5.1.1, that the $\mathcal{GGIW}$ model is a method that estimates the target properly. However, visual inspection is not a valid evaluation tool, and a more robust metric needs to be applied, for instance, the Gaussian Wasserstein Distance.

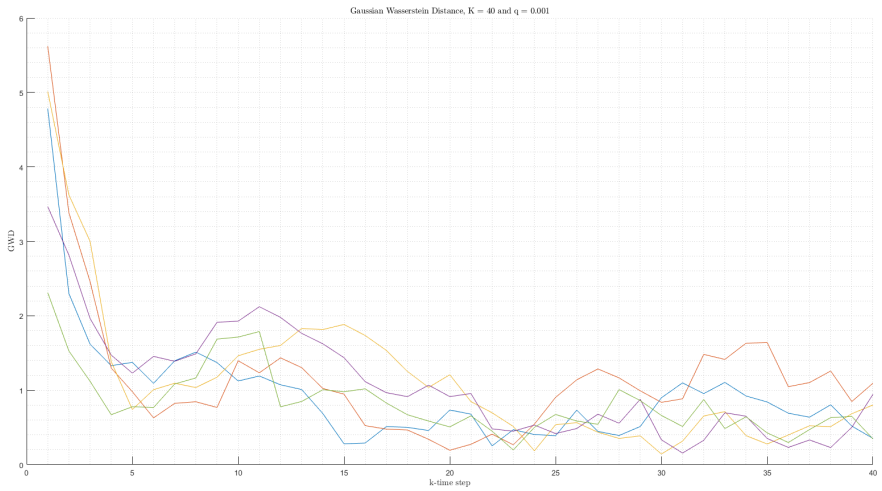

(a) Gaussian Wasserstein Distance for q = 0.001.

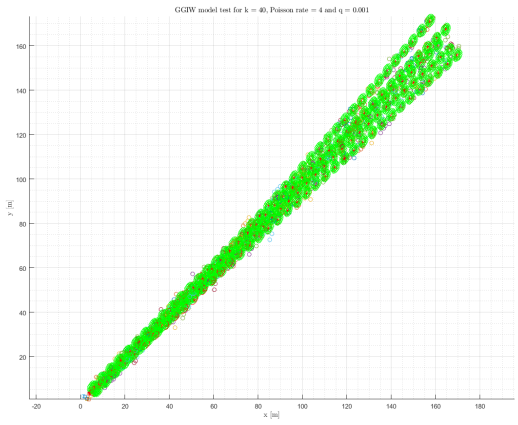

(b) $\mathcal{GGIW}$ for q = 0.001.

Figure 5.1.2: $\mathcal{GGIW}$-GWD evaluation environment.

In order to check that the single extended target is working, several iterations have been run with the same prior knowledge, as it is done in a Monte Carlo simulation; and the trend of the GWD metric analyzed. The setting values of the initial knowledge can be found in Appendix C: Parameters values. From the

fig.5.1.2a, one could assess the performance of the $\mathcal{GGIW}$ model. Note that there are more plots attached to the Appendix B describing different process noise and the corresponding *GWD* metric.

If the *GWD* iterations curves are averaged, it could be possible to note that the metric tends to a stationary value[2], below 2, with time steps. This trend is natural of two similar probability density functions since both real and estimated extensions and positions converge to the same values. The same solution can be deduced from the eq. 4.2, where the equation tends to a stationary value when the positions and the extensions of the real and estimate targets share the same value. Therefore, the employed method for single extended target can be said to be appropriate to describe the tracking environment.

5.1.2 Multiple targets scenario

Once the single extended target performance was analyzed and its evaluation addressed, as shown in the previous section, the multiple targets scenario was studied. Note here that one of the main objectives of the project is to test the algorithm on a real urban scenario, hence these first assessment steps are done on grounds of ensuring that the PMBM filter is working properly. Here, the reader should recall the described *GOSPA* metric, based on *GWD* and penalizations.

For the simulation environment 10 time step estimates were run and shown with specific parameters describing the birth. The purpose of this simulation was to test different types of targets within the FoV, this is, stationary and moving objects within the area under analysis. In the simulated scenario, 1 non-stationary object and 2 stationary objects were analyzed. The associated parameters values can be found in the Appendix C. Please note that the ego-vehicle is driven through the analyzing objects.

The multiple hypotheses oriented method carried from time step to time step different hypotheses, different Multi-Bernoullis, and their corresponding weights. The objects estimates shown in the following figures are only representative of the most likely hypothesis, after being selected from a table of weights/global hypotheses that were derived from the most likely previous time step global hypotheses. In the case of these simulations, the amount of global hypotheses $\mathcal{H}_{N'}$ was set to $N' = 10$. Later, this approach was changed to a probability thresholding, using probability of death. Note again that even if the most likely hypothesis is

[2]The GWD is unit less, this is, the distance is between two probability functions, thus no unit assigned to this comparison.

depicted, the derivation took all the previous time step global hypotheses into account, enclosing inside all previous global hypotheses.

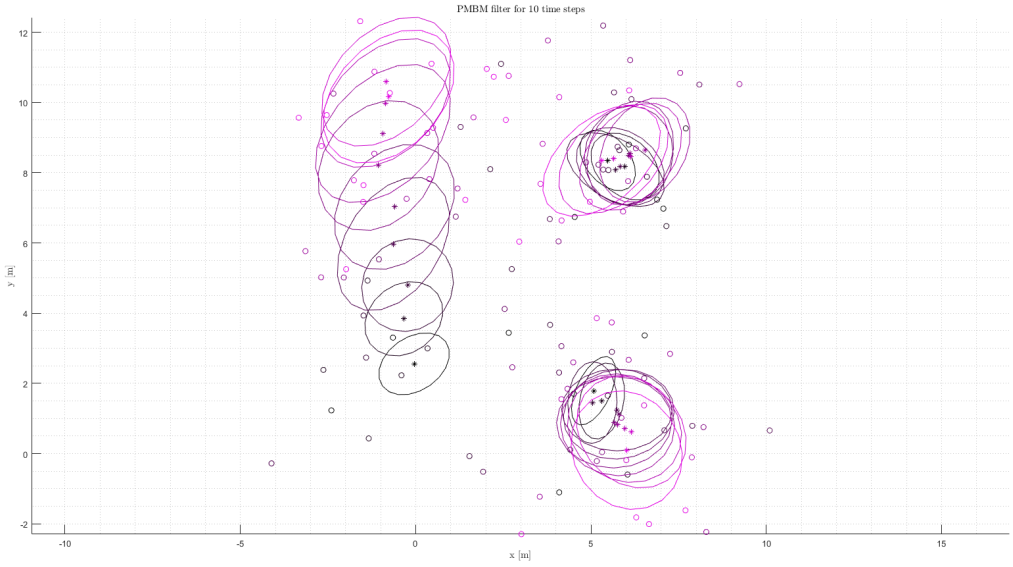

Figure 5.1.3: Multiple targets estimates.

In fig. 5.1.3, the estimates of the three targets can be seen throughout the 10 time steps. In order to make it understandable, different levels of colours have been used, from the starting or initial estimates coloured in black, to the ending of the estimates or tracking, coloured in violet. If one takes a close look at the extensions, increases on the three targets extensions during the time could be seen.

The extents trends, directly dependant on the degrees of freedom and covariance of the Inverse Wishart distributions, grow until they reach close values to the real extensions, this is, $w = 3$ m, $l = 3$ m. The following extensions are the trends of the shapes estimates and give the visual representation of what it has been commented (the next examples follows the notation X_k^{Obj}):

$$X_1^1 = \begin{pmatrix} 1.0173 & 0.2920 \\ 0.2920 & 0.7789 \end{pmatrix} \quad X_1^2 = \begin{pmatrix} 0.3984 & 0.3399 \\ 0.3399 & 0.9526 \end{pmatrix} \quad X_1^3 = \begin{pmatrix} 0.6288 & -0.283 \\ -0.283 & 0.7443 \end{pmatrix}$$

$$X_5^1 = \begin{pmatrix} 2.9526 & 0.8381 \\ 0.8381 & 3.1897 \end{pmatrix} \quad X_5^2 = \begin{pmatrix} 2.4995 & 0.1439 \\ 0.1439 & 1.6372 \end{pmatrix} \quad X_5^3 = \begin{pmatrix} 1.6049 & 0.0979 \\ 0.0979 & 1.9830 \end{pmatrix}$$

$$X_{10}^1 = \begin{pmatrix} 3.51 & 1.3334 \\ 1.3334 & 3.6186 \end{pmatrix} \quad X_{10}^2 = \begin{pmatrix} 2.5273 & -0.320 \\ -0.320 & 2.8648 \end{pmatrix} \quad X_{10}^3 = \begin{pmatrix} 2.8225 & 1.2359 \\ 1.2359 & 2.4951 \end{pmatrix}$$

It can be seen that the estimates of the extensions tend to the real extensions with time-steps. As a fact, an important check point of the used theory can be seen in the previous set of matrices where the positive semi-definite values are shown, describing the lengths and orientations of any Gaussian shape or extension of any target.

In order to verify what it has been shown, the next fig. 5.1.4 has been introduced. It gathers both the *GOSPA* values and the weights linked to the most likely Multi-Bernoullis. As it happens with the Gaussian Wasserstein Distance, the pattern of this last metric tends to reduce with time steps. For instance, in this particular simulation environment, the evaluation metric stays around the value 10, a positive result since *GOSPA* is calculated taking into account the three real objects, false and missed targets alarms. The weights tend to the value ≈ 0.15, which might have happened due to the convergence of the SO algorithm into the same association space.

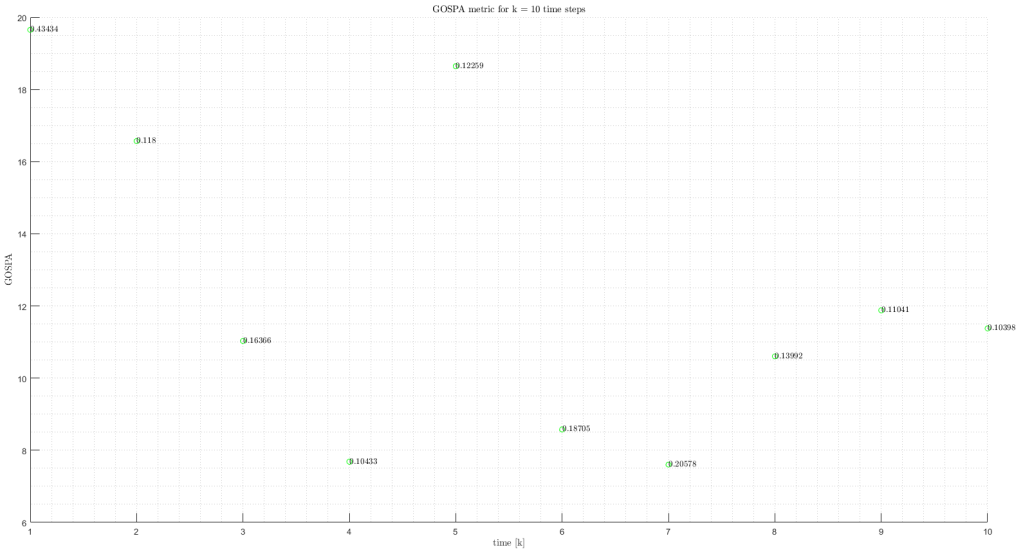

Figure 5.1.4: *GOSPA* values and most likely global hypothesis weights.

As for the time step $k = 5$, a peak in the *GOSPA* value appears. When the *GOSPA* algorithm was analyzed, a penalization term was introduced that offered the possibility of analyzing and in case penalizing objects that are not under some set conditions. It is thought that there might be two reason why the commented peak appeared, the first and not most probable one related to the presence of a false or missed detections (which should appear in fig. 5.1.3, but are not found)

and the second one, which is supported by the extension X_5^2, X_5^3, related to the estimates, which are not close compared to the actual targets.

Therefore, taking into consideration everything analyzed before, the simulation environment that represents a scenario with multiple targets within can be said to be tracked properly with the Poisson Multi-Bernoulli Mixture filter.

5.2 Real Scenarios

Everything described, analyzed and evaluated up until this point supported the efficiency of the PMBM filter and its robustness when it comes to track dense scenarios clustered with both stationary and non-stationary objects. Both *GWD* and *GOSPA* metrics offered the possibility to compare the ground truth with the estimated ones, allowing us to continue with the method used in this project.

Since the final aim of technology might be the use and implement of itself in the market, the testing associated to a real scenario or environment comes sensible and compulsory. The same filter should work efficiently in both environments and that is the reason why it is important to run the same implementation with some real measurements. Moreover, this will allow also to time the filter and give some insights about the processing time of the estimates.

For the same real measurements, several initializations were set: the ones related to the Gauss distribution and the ones related to the Inverse-Wishart distribution.

The commented real scenario can be depicted as below:

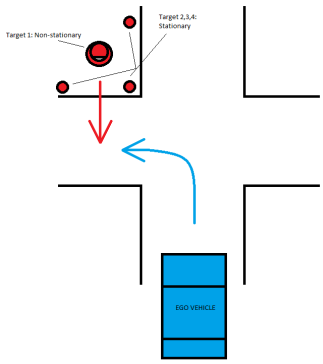

Figure 5.2.1: A snippet of the real situation.

5.2.1 1^{st} Approach: Certainty in the Position of the Birth

In the following figure, the reader could see how the PMBM filter tracked the 4 objects throughout the recording time. Note once again the difference in colour, representing black initial estimates and changing towards light violet by the end of the tracking; the stars painted in blue represent the real measurements. Please, find the initial birth values in the Appendix C.

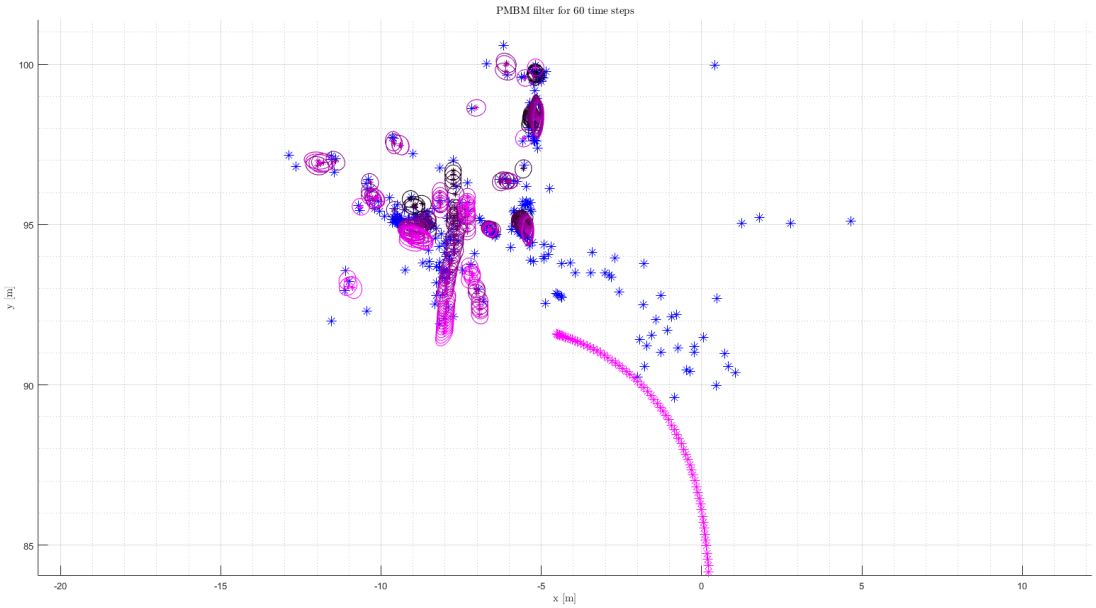

Figure 5.2.2: 1^{st} approach with real measurements.

Several things have to be pointed out and analyzed from the fig. 5.2.2. For instance, the spurious measurements on the crossroad. For the full representation of the reality, the spurious have been left depicted, but before running the filter over the presented scenario some pre-filtering has been applied on the commented measurements; filtering them out[3].

The ellipses or extents around the real targets, shown in fig. 5.2.2, belong to the group of false targets or alarms and it is thought that the presence of them might be motivated by the tuning of the location of the real measurements and the size of the selected extensions; being the measurements associated more to false alarms than to the real targets. These false alarms are filtered out once their accumulated probability of existence reach a value below the probability of death.

[3]This spurious filtering can be done by using signal processing combined with radar theory

As for the real objects, the 4 main targets are visible in the figure above. These targets, depending on their nature, stay or move throughout the time. This is the case of the pedestrian or object found within the 3 pillars and that crosses the crosswalk by the time the vehicle reaches the crosswalk.

Notice on the pedestrian track, the appearance of two branches around the XY-position[4]: $(x, y) = (-7, 94)$. This event could be explained by the fact that the radar beam reflected firstly on the road and came back to the sensor. It could be verified by the use of the measurements back-scattered intensities; where twice reflected[5] intensity being lower than the one directly measured form the pedestrian in the LOS[6]. Unfortunately, there is no function in charge of the measurement intensities, thus there is no possibility to rearrange these first estimates in a more sensible and efficient way.

5.2.2 2^{nd} Approach: Uncertainty in the Location of the Birth

With the birth parameters found in the Appendix C, the following estimates can be obtained for an uncertain birth initialization:

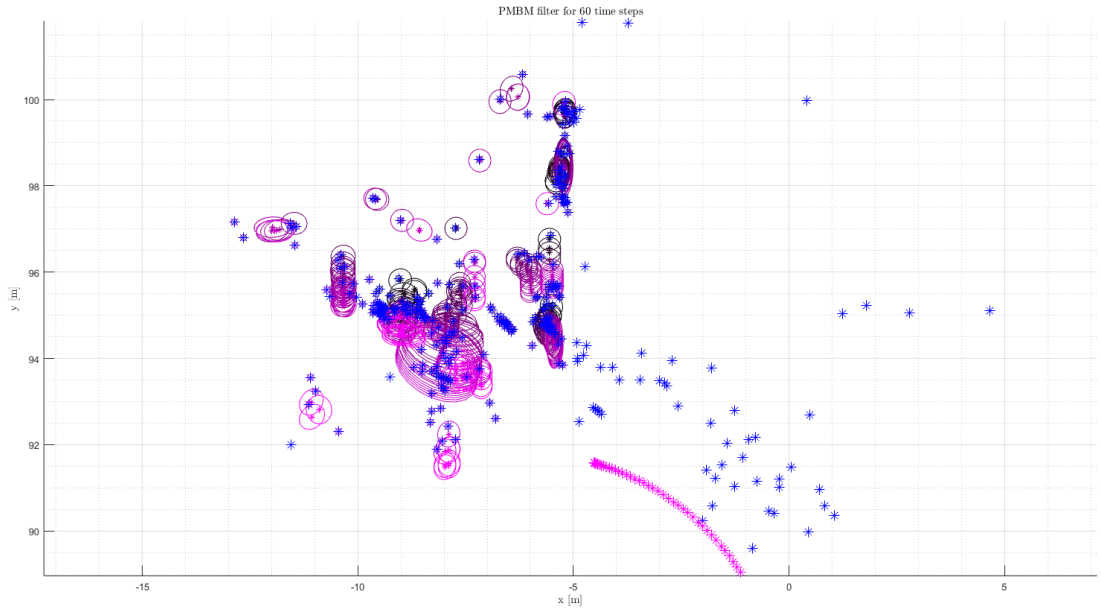

Figure 5.2.3: 2^{nd} approach with real measurements.

[4]In metres.
[5]First bounce on the pedestrian and second on the road.
[6]Line-of-Sight.

From the previous fig. 5.2.3, several things can be understood. For this particular scenario, the birth has been set to be the same for the four objects with a large uncertainty. This tuning is not the best one as it can be deduced from the figure above, since the targets do not get estimated as they should (for instance, the pedestrian estimates). If one compared the estimates obtained here with the ones shown in fig. 5.2.2, two important things could notice. First that the extensions do not represented faithfully the actual objects and second that the tracking of this moving object seems to be delayed compared to the real measurements. One of the reasons why this could happen is the way the initial parameters were set. Since the configuration of the scenario can change drastically tuning slightly the commented parameters, the estimates do not reach close values. This tuning fact, as it will be explained later, will be a sensitive factor that will require further work.

5.2.3 Lower the Initial Extensions Values

Up until now, the changes have been applied over the location and uncertainty on it. Since the parameters cover also other two distributions, Poisson and Inverse Wishart, the tuning of the other two distributions were thought to be run to see different results. Note here that the Gamma function, dependant on the Poisson rate, did not changed due to the already suitably selected parameters.

The information about the initial states is limited, but the nature of the real targets is given by the data provider, this is, there are 4 targets in the landscape where 3 are pillars and 1 is a pedestrian. The sizes of the initial extensions introduced to the births should be sensible or follow the characteristics of the targets under analysis. The next two analysis gather two initializations for the IW conjugate prior distribution: 2 different and smaller initial extensions compared to fig. 5.2.2. These differences in the initialization of the stationary[7] and non-stationary objects, are set to be[8]:

$$X_1 \approx \begin{pmatrix} 0.5 & 0 \\ 0 & 0.5 \end{pmatrix}$$

$$X_2^{Stat} \approx \begin{pmatrix} 0.25 & 0 \\ 0 & 0.25 \end{pmatrix}$$

$$X_2^{NStat} \approx \begin{pmatrix} 0.5 & 0 \\ 0 & 0.35 \end{pmatrix}$$

[7] Same objects, which one could deduced that they share the same extension.

[8] The following X_2 are deduced approximately from regular pillars and average man found on the streets.

5.2.4 3^{rd} Approach: X_1, X_2^{Stat} and X_2^{NStat} Extensions and Certainty in the Location of the Birth

The obtained estimates are shown below. The colours follow the same meaning as the ones used in the previous analysis.

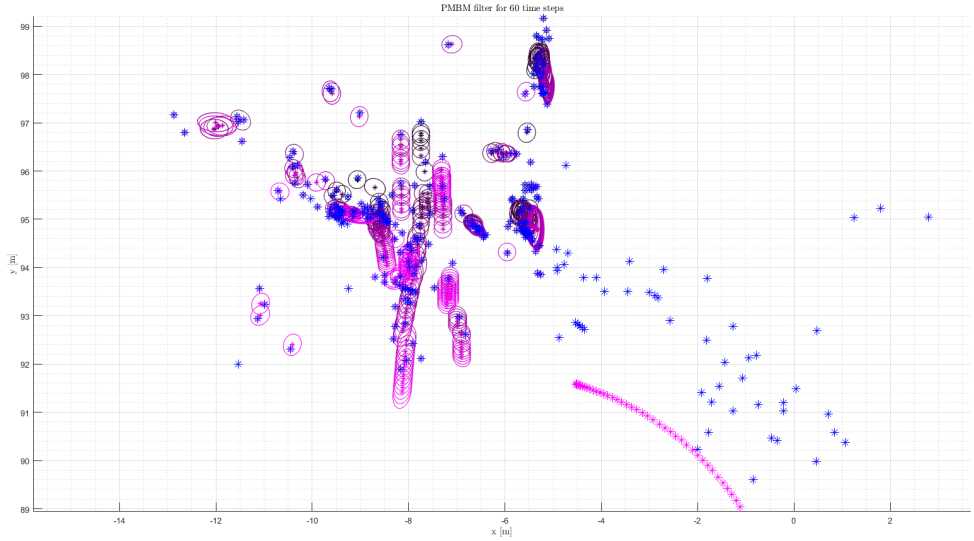

Figure 5.2.4: Same X_1 extensions for the 4 objects with the birth initial values of Appendix C.

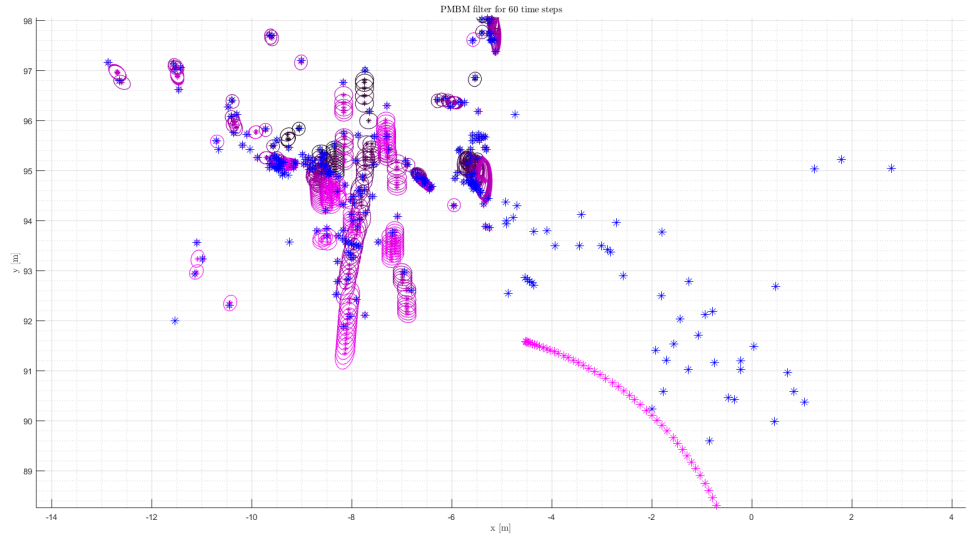

Figure 5.2.5: X_2 extensions with the birth initial values of Appendix C.

From the set of figures above, some minor improvements compared to the 1^{st}-approach can be seen.

5.2.5 4^{th} Approach: X_1, X_2^{Stat} and X_2^{NStat} Extensions and Uncertainty in Birth

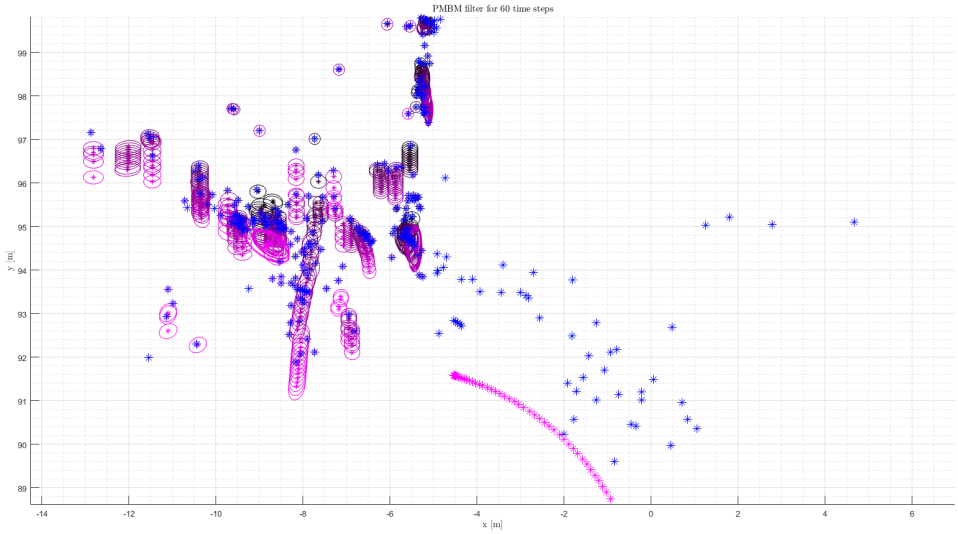

Figure 5.2.6: X_1 and X_2 extensions for the objects with uncertainty in the birth initial values of Appendix C.

There is an improvement in the tracking of the FoV that is thought to be partially caused by the extensions employed, even having used the same uncertainty in both birth positions and covariances of the objects. These estimates, with high uncertainty in the initial parameters, are thought to be the best estimate of all the sets analyzed if one compares the used parameters and the results.

A common event happening in all approaches is the coasting[9]. If the target, either false alarm or real one, does not acquire or is associated to any measurement, the filter will react and perform the correction or update accordingly with update without any measurement. In the case of this filter, with the function found in the table X in [6, p. 9].

Therefore, the filter reacts better to these last initialization parameters, highlighting the robust performance of the filter under particular and sensible initial-

[9]Targets with no detections assigned.

izations such as uncertainty in the positions but not in the extent sizes.

5.2.6 Timing

This section is committed to give the necessary timing that is required to run 60 time-step scenarios with the implemented code.

Timing 1^{st} approach [s]
- MAIN: 201,436
- INITIALIZATION OBJECTS (IO): 0,004
- BUILD
  - Sb-init: 0,003
- PREDICT-UPDATE: 199,298
  - update-pmbm-MH: 199,096
    - Object Copy: 120,845
    - InitializeSO: 31,142
    - SO algorithm: 14,771
- GGIW: 26,369

Timing 2^{nd} approach [s]
- MAIN: 208.71
- INITIALIZATION OBJECTS (IO): 0,004
- BUILD
  - Sb-init: 0,003
- PREDICT-UPDATE: 205,779
  - update-pmbm-MH: 205.577
    - Object Copy: 123,996
    - InitializeSO: 27,805
    - SO algorithm: 13,585
- GGIW: 30,881

Timing 3.1 approach [s]
- MAIN: 310.052
- INITIALIZATION OBJECTS (IO): 0,004
- BUILD
  - Sb-init: 0,003
- PREDICT-UPDATE: 305,435
  - update-pmbm-MH: 305,214
    - Object Copy: 214,215
    - InitializeSO: 46,445

```
        SO algorithm:  17,520
    GGIW: 33,243

  Timing 3.2 approach [s]
    MAIN: 379,738
    INITIALIZATION OBJECTS (IO): 0,004
    BUILD
      Sb-init:  0,003
    PREDICT-UPDATE: 374,795
      update-pmbm-MH: 305,214
        Object Copy:  252,420
        InitializeSO: 55,093
        SO algorithm:  10,021
    GGIW: 36,467

  Timing 4th approach [s]
    MAIN: 368,455
    INITIALIZATION OBJECTS (IO): 0,004
    BUILD
      Sb-init:  0,003
    PREDICT-UPDATE: 363,830
      update-pmbm-MH: 363,582
        Object Copy:  260,150
        InitializeSO: 57,918
        SO algorithm:  20,103
    GGIW: 36,780
```

Where the most critical function takes the following times to process:

Critical timing values for Predict-Update				
1^{st}	2^{nd}	3.1	3.2	4^{th}
199.096	205.779	305.435	374.795	363.830

and the timing of both initialization of the SO and the SO, respectively:

Timing for the InitializeSO and SO				
1^{st}	2^{nd}	3.1	3.2	4^{th}
31.142	27.805	46.445	55.093	57.918
14.771	13.585	17.520	10.021	20.103

Chapter 6

Discussion

The results shown in the previous section, both derived from simulated scenarios and from real scenarios, describe the way the Poisson Multi-Bernoulli filter performs; highlighting the robustness of the filter when it comes to tracking multiple and different kinds of objects, stationary and non-stationary ones.

The first results committed to the simulated scenarios validate the performance of the filter through metrics like the *GWD* and *GOSPA*. It is shown that the algorithm presented is an appropriate method to track dense environments.

The single extended target model was tested; running it for several iterations and showing us that the *Gaussian Wasserstein Distance* tends to a low and stationary value, making us continue with the multiple target scenarios. Furthermore, other characteristics of the single extended target are confirmed to work suitably, such as the measurements likelihood that is dependant on the normal distribution (please, see the Appendix B for complementary figures) or the extensions estimates (including the proper orientations).

As for multitarget simulations, the errors obtained by the *GOSPA* method tell us that the filter gets to a point where the estimates get closer to the real targets. Note that this *GOSPA* metric, based in *GWD*, needs ground truth to be employed. However, the real scenario evaluation lack of this ground truth. This non-existing real ground truth can be mitigated assuming that if the implementation and evaluation of the simulated environments have reached the correct performance assessment, then the performance assessment of real scenarios will be also achieved, provided that no changes in the code have been made between these two environments. It is a vague assumption at first glance, but for this master thesis length and referring to the results, one could assume and motivate it. Once again, *only*

if the same procedures and codes have been used.

In this section another crucial outcome is deduced, common of all tracking filters, this is, the importance of the tuning of the filter and which leads us to one important aspect related to the PMBM filter: the sensitiveness of the initial parameters. Notice that the initial values are introduced to a specific distribution, the Gaussian Normal distribution, that might not be the suitable one to describe situations where uncertainties are spread in a uniform way, for instance, initialization of the tracking space or FoV.

In order to improve this, further steps could be taken such as implementing the initialization with a uniform distribution. This would weigh everything within the area of events with the same probability of occurrence. Moreover, there is always the possibility to employ the trial-and-error concept over all parameters and, once converged, provide these parameters values. Parameters such as the ones related to probabilities (p_s, p_D and p_{Death}) can be also studied and tuned, but they have been left out of this project even if they represent an important group to examine. We could use these parameters and tailor the filter to the FoV, which might not be the most general approach to follow but it might be adequate if some pre-processing is run before this PMBM filter.

As for the false alarms that appear in both simulated and real scenarios, they form a critical aspect to analyze since they can lead to an overall bad performance of the filter, as shown in a previous approach. It is thought that if these false alarms were studied deeper and combined or arranged together in some specific way under some existing and proved theory, for instance combining in and penalizing (as in *GOSPA*) the probabilities of existence and the behaviour of the false alarms inside FoV, the filter would improve its performance in both time and efficiency. For example, the associations are dependant on the amount of targets and the false alarms are part of the targets that the filter runs. Therefore, a more sensible grouping/merging of the commented targets set would contribute to the improvement of the filter.

A merging step appears in the stochastic optimization to the radar data, where measurements are arranged and grouped with targets and weighted with belonging likelihoods. A possible approach, as it is done with the initialization of the DA, could be to extend this idea and run the filter firstly estimating everything inside the FoV, up to some extent, and secondly narrowing what it is estimated with another algorithm that clusters or merges with available information. The necessary data such as likelihoods, weights and states is already accessible and can

be reemployed in most of the procedures above. Although this would increase the timing, it is thought that it will help to relieve the burden and repetitiveness that might happen throughout the PMBM filter such as false alarms and assignment space convergence.

Regarding the timing, further work could be addressed. If we take a look in the timing section and the tables, we will see a procedure that needs more time than it should take. According to some survey made in the office where the project was set, the time needed to process the estimate of one time step data should be around: $\Delta t_{\text{Estimate time}} \approx \frac{\Delta t_{\text{Real time}}}{10}$.

It is obvious from the commented section that the timing of the procedure is not matching the previous rule of thumb. Taking a look at the values, most of the time spent was in the function "Object Copy", an important function when it comes to hold and analyze all the targets within the FoV. An approach to solve the problem would be to work on this function and make it more time-efficient or changing it with a faster method that allows to work with Matlab `handle`-object class.

Chapter 7

Conclusion

The main idea behind the project was to solve a dense scenario, for instance, an urban landscape in a simultaneous or real-time mode. Moreover, there was another difficulty describing the nature of the objects within the scenario, being stationary or non-stationary.

Among all possible filters available in the market that give a reasonable solution, The Poisson Multi-Bernoulli Mixture has been selected, studied and employed throughout this project; which copes with both simulated and real scenarios and is based solidly in strong mathematical foundations. The performance is further enhanced with the combination of suitable models that describes the objects within the scenario or FoV. The filter overcomes the problem of the dense FoV problem efficiently.

One of the main conclusions after having done the project is the importance on merging strong mathematical tools such as the implementation of theories like conjugate priors, stochastic optimization and multiple hypotheses in order to solve problems such as dense urban scenarios. It has been demonstrated how combining these concepts and ideas, the problem was possible to be defined and meaningful results were obtained. Moreover, the multiple hypotheses tracking gave a new approach to the conventional tracking method, improving the performance with the weighing and pruning of the branches through probability.

All over this thesis, the studied algorithm has been thought to be implemented particularly for the vehicle industry, but as the reader might already sense, the same theory that was derived by developments in the sensors industry can now be introduced and employed in a more global market such as in surveillance situations for airport control, in biology for cells reproducibility control or in any random

and clustered 3D environment for objects estimation.

Therefore, the combination of stochastic theories that enable to describe random processes such as the ones applied in this project scenarios is thought to give considerable and pioneer solutions to the Autonomous Driving business.

Bibliography

[1] David Arthur and Sergei Vassilvitskii. "K-means++: The Advantages of Careful Seeding". In: *Proceedings of the Eighteenth Annual ACM-SIAM Symposium on Discrete Algorithms*. SODA '07. New Orleans, Louisiana: Society for Industrial and Applied Mathematics, 2007, pp. 1027–1035. ISBN: 978-0-898716-24-5. URL: http://dl.acm.org/citation.cfm?id=1283383.1283494.

[2] Aurlien Bellet et al. *Metric learning*. English. 1st ed. Vol. Number 30. San Rafael, California: Morgan and Claypool Publishers, 2015.

[3] M. Feldmann, D. Franken, and W. Koch. "Tracking of Extended Objects and Group Targets Using Random Matrices". In: *IEEE Transactions on Signal Processing* 59.4 (Apr. 2011), pp. 1409–1420. ISSN: 1053-587X. DOI: 10.1109/TSP.2010.2101064.

[4] Karl Granström, Marcus Baum, and Stephan Reuter. "Extended Object Tracking: Introduction, Overview, and Applications". In: *JAIF* 12.2 (December 2017).

[5] Karl Granström, Maryam Fatemi, and Lennart Svensson. "Gamma Gaussian Inverse-Wishart Poisson Multi-Bernoulli filter for extended target tracking". In: *FUSION 2016 - 19th International Conference on Information Fusion, Proceedings*. 2016, pp. 893–900. ISBN: 978-0-9964-5274-8.

[6] Karl Granström, Maryam Fatemi, and Lennart Svensson. "Poisson multi-Bernoulli conjugate prior for multiple extended object estimation". In: abs/160506311 (2016).

[7] K. Granström et al. "Likelihood-based data association for extended object tracking using sampling methods". In: *IEEE Transactions on Intelligent Vehicles* PP.99 (2017), pp. 1–1. ISSN: 2379-8858.

[8] K. Granström et al. "Pedestrian tracking using Velodyne data - stochastic optimization for extended object tracking". In: (June 11-14, 2017), pp. 39–46. DOI: 10.1109/IVS.2017.7995696.

[9] J. W. Koch. "Bayesian approach to extended object and cluster tracking using random matrices". In: *IEEE Transactions on Aerospace and Electronic Systems* 44.3 (July 2008), pp. 1042–1059. ISSN: 0018-9251. DOI: 10.1109/TAES.2008.4655362.

[10] Solomon Lefschetz and De Gruyter (e-book collection). *Introduction to Topology*. English. Princeton, NJ: Princeton University Press, 2016;2015;

[11] Ronald Maher. "A survey of PHD filter and CPHD filter implementations". English. In: vol. 6567. SPIE, 2007. Chap. 1, 65670O-65670O-12. ISBN: 0277-786X.

[12] Ronald P. S. Mahler. *Statistical Multisource-Multitarget Information Fusion*. Norwood, MA, USA: Artech House, Inc., 2007. ISBN: 1596930926, 9781596930926.

[13] Scott L. Miller et al. *Probability and random processes: with applications to signal processing and communications*. English. 2nd.;Second; Boston, MA: Academic Press, 2012. ISBN: 9780123869814;0123869811;

[14] Abu S. Rahmathullah, Angel F. Garcia-Fernandez, and Lennart Svensson. "Generalized optimal sub-pattern assignment metric". English. In: (July 10-13, 2017).

[15] D. Schuhmacher, B. -. Vo, and B. -. Vo. "A Consistent Metric for Performance Evaluation of Multi-Object Filters". English. In: *IEEE Transactions on Signal Processing* 56.8 (2008), pp. 3447–3457.

[16] L.D. Stone et al. *Bayesian Multiple Target Tracking, Second Edition:* Radar/Remote Sensing. Artech House, 2013. ISBN: 9781608075539. URL: https://books.google.se/books?id=fJhQAgAAQBAJ.

[17] Roy L. Streit. *Poisson Point Processes: Imaging, Tracking, and Sensing*. German. 1. Aufl. Springer Science + Business Media, 2010.

[18] Chalmers Univerity of Technology. *First self-driving bus in operation at Chalmers*. URL: https://www.chalmers.se/en/areas-of-advance/Transport/news/Pages/First-self-driving-bus-in-operation-at-Chalmers.aspx (visited on 05/29/2018).

[19] Carnegie Mellon University. *Navlab: The Carnegie Mellon University Navigation Laboratory*. URL: http://www.cs.cmu.edu/afs/cs/project/alv/www/index.html (visited on 05/29/2018).

[20] S. Yang, M. Baum, and Karl Granstrom. "Metrics for performance evaluation of elliptic extended object tracking methods". In: Sep 19-21, 2016.

Appendix A

Pseudo-code/Flow-chart

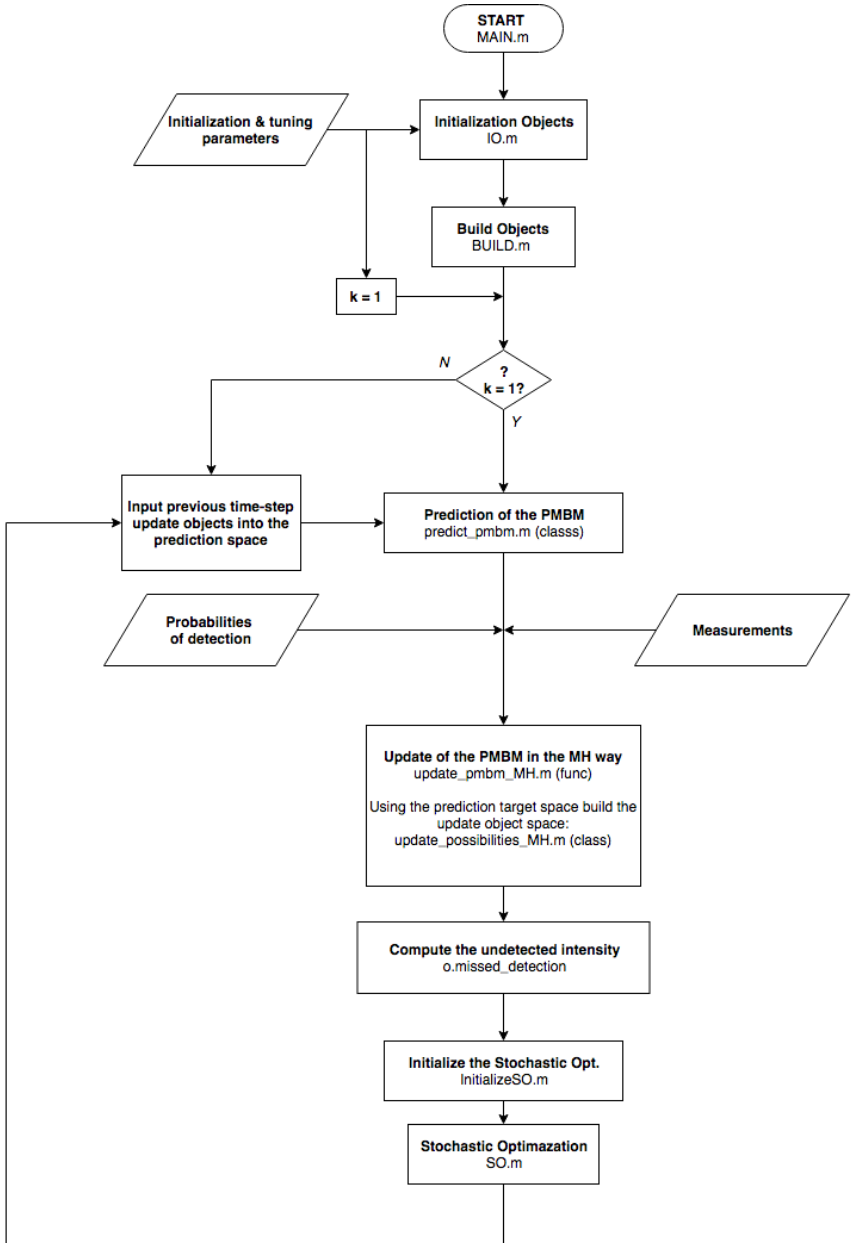

Figure A.0.1: Flow-chart. Snippet 1

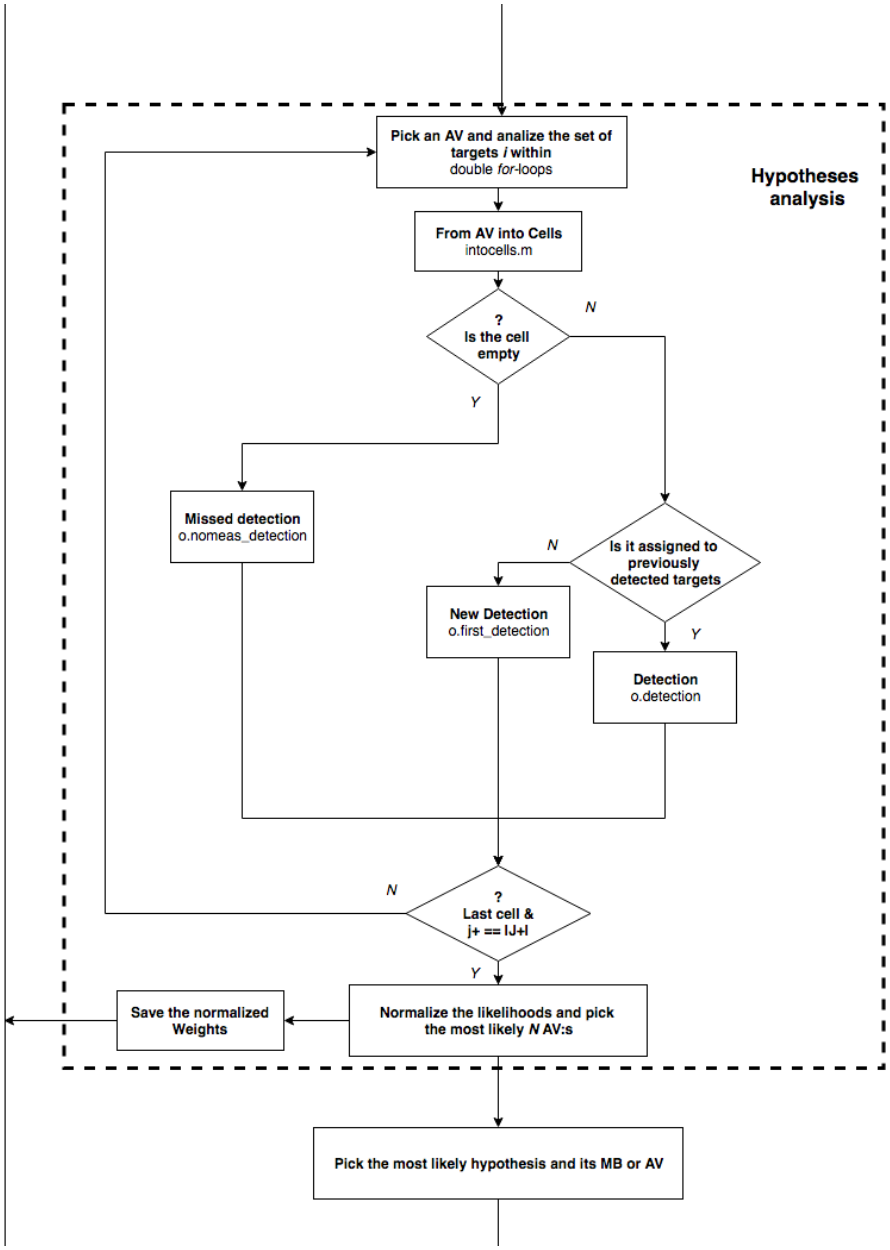

Figure A.0.2: Flow-chart. Snippet 2

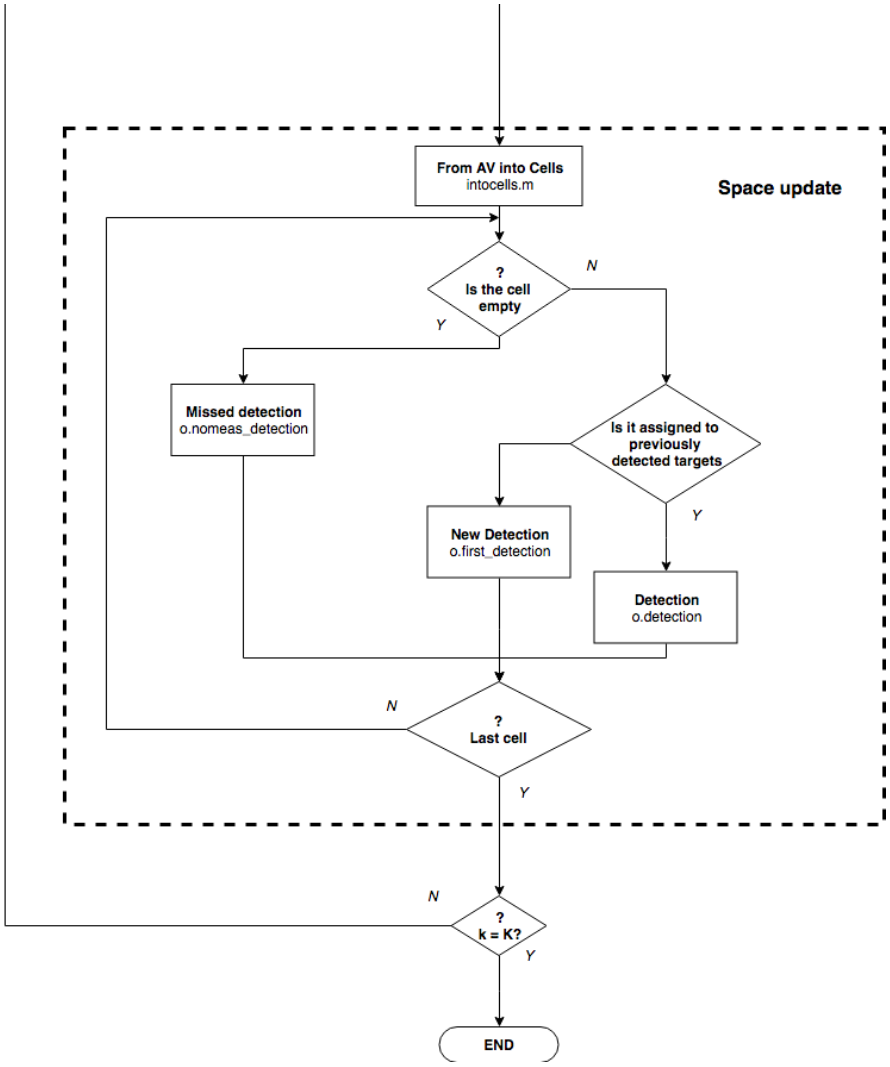

Figure A.0.3: Flow-chart. Snippet 3

Appendix B

Complementary figures for evaluation

B.1 Simulated Environments

B.1.1 Single Extended Target - GWD

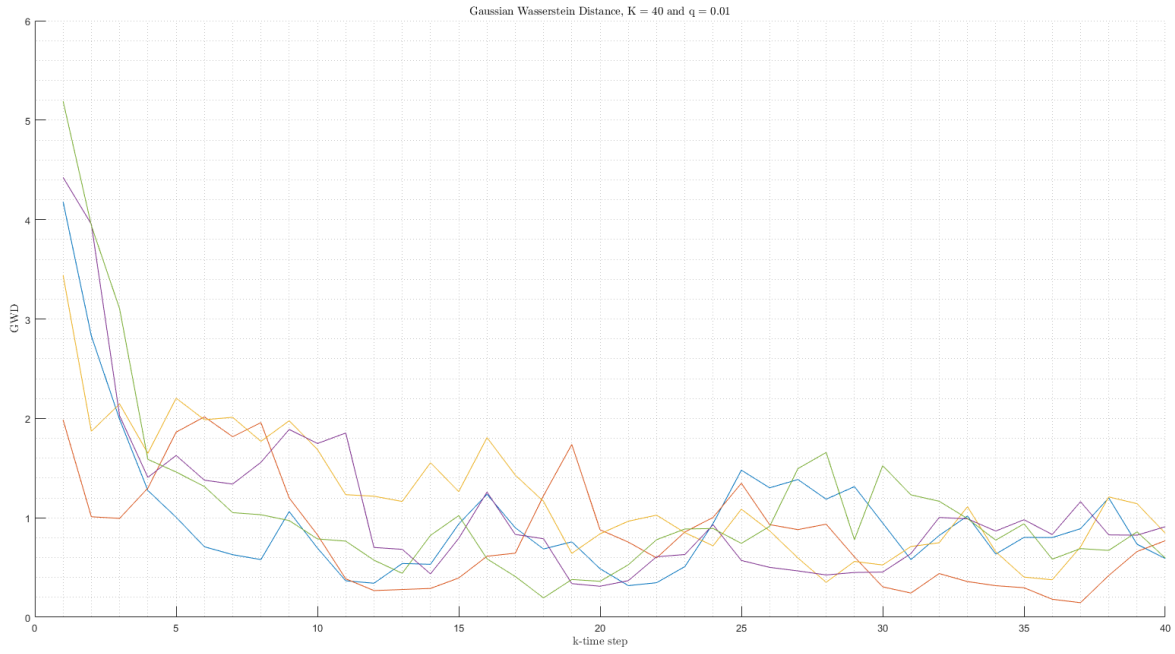

Figure B.1.1: Gaussian Wasserstein Distance for q = 0.01.

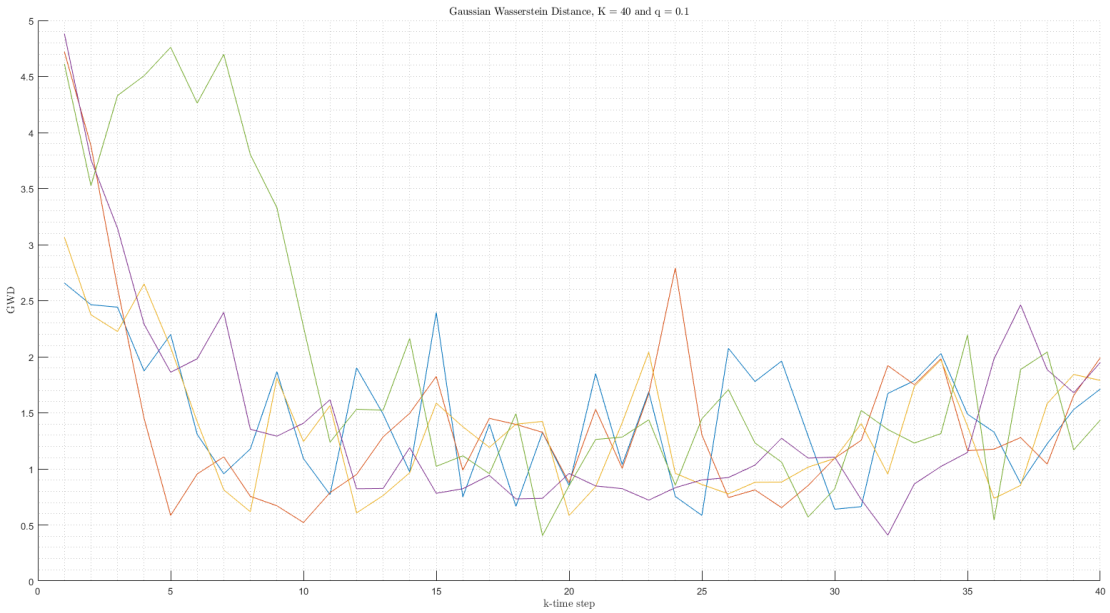

Figure B.1.2: Gaussian Wasserstein Distance for q = 0.1.

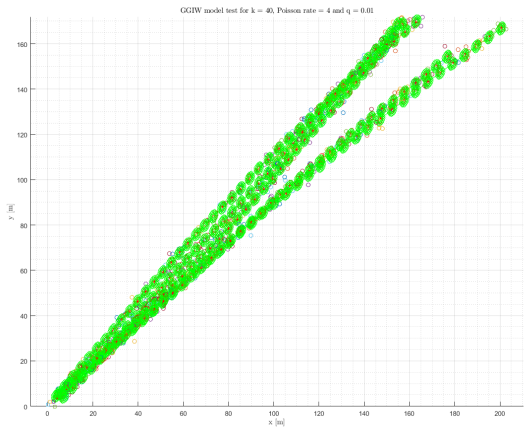

(a) $\mathcal{GGIW}$ for q = 0.01.

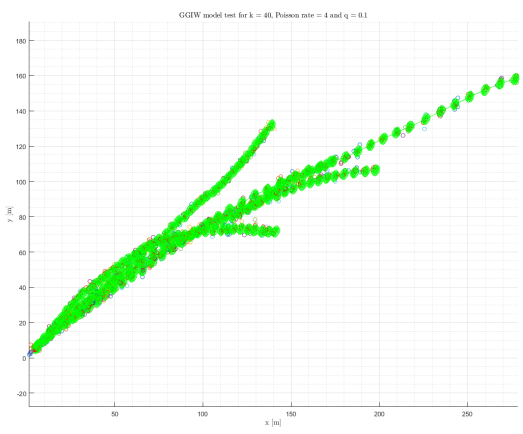

(b) $\mathcal{GGIW}$ for q = 0.1.

B.1.2 Single Extended Target - Measurements distribution

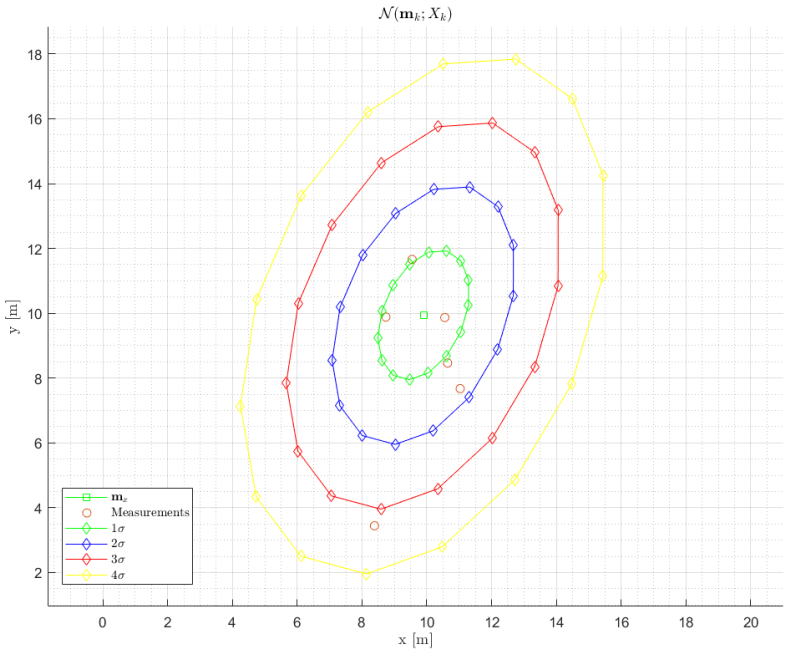

Figure B.1.3: Measurements distribution.

Appendix C

Parameters values

C.1 Simulated Environments

C.1.1 Single Extended Target

GGIW birth initial parameters	
Parameter	**Value**
α	25
β	5
$\mathbf{m}$	$\begin{pmatrix} 2 & 2 & 4 & 4 \end{pmatrix}$
P	$\text{diag}[\begin{pmatrix} 1 & 1 & 0.1 & 0.1 \end{pmatrix}^2]$
v	20
V	$\begin{pmatrix} 2 & \frac{\mathbf{m}_4}{\mathbf{m}_3} \\ \frac{\mathbf{m}_4}{\mathbf{m}_3} & 4 \end{pmatrix}$
q	$\begin{pmatrix} 0.001 & 0.01 & 0.1 \end{pmatrix}$
η	4
τ	5

C.1.2 Multiple targets scenario

GGIW birth initial parameters	
Parameter	**Value**
α	25
β	5
$\mathbf{m}_1$	$\begin{pmatrix}0 & 0 & 0 & 1\end{pmatrix}^T$
$\mathbf{m}_2$	$\begin{pmatrix}5 & 2 & 0 & 0\end{pmatrix}^T$
$\mathbf{m}_3$	$\begin{pmatrix}5 & 9 & 0 & 0\end{pmatrix}^T$
P	$\text{diag}[\begin{pmatrix}0.1 & 0.1 & 0.1 & 0.1\end{pmatrix}^2]$
v	20
V	$\begin{pmatrix}3 & 0\\ 0 & 3\end{pmatrix}$
q	0.001
η	4
τ	5

C.2 Real scenarios

C.2.1 Multiple targets scenario

1^{st} approach

GGIW birth initial parameters	
Parameter	**Value**
α	8
β	2
$\mathbf{m}_1$	$\begin{pmatrix}-9.5 & 95 & 0 & 0\end{pmatrix}^T$
$\mathbf{m}_2$	$\begin{pmatrix}-6 & 95 & 0 & 0\end{pmatrix}^T$
$\mathbf{m}_3$	$\begin{pmatrix}-5 & 99 & 0 & 0\end{pmatrix}^T$
$\mathbf{m}_4$	$\begin{pmatrix}-8 & 95 & 0 & -1\end{pmatrix}^T$
P	$\text{diag}[\begin{pmatrix}1 & 1 & 0.1 & 0.1\end{pmatrix}^2]$
v	20
V	$\begin{pmatrix}1 & 0\\ 0 & 1\end{pmatrix}$
q	0.1
η	4
τ	10

2^{nd} approach

GGIW birth initial parameters	
Parameter	**Value**
α	8
β	2
$\mathbf{m}_1$	$\begin{pmatrix}-7 & 97 & 0 & 0\end{pmatrix}^T$
$\mathbf{m}_2$	$\begin{pmatrix}-7 & 97 & 0 & 0\end{pmatrix}^T$
$\mathbf{m}_3$	$\begin{pmatrix}-7 & 97 & 0 & 0\end{pmatrix}^T$
$\mathbf{m}_4$	$\begin{pmatrix}-7 & 97 & 0 & -1\end{pmatrix}^T$
P	$\text{diag}[\begin{pmatrix}2 & 2 & 0.1 & 0.1\end{pmatrix}^2]$
v	20
V	$\begin{pmatrix}1 & 0\\ 0 & 1\end{pmatrix}$
q	0.1
η	4
τ	10

3.1 **approach**

GGIW birth initial parameters	
Parameter	**Value**
α	8
β	2
$\mathbf{m}_1$	$\begin{pmatrix}-9.5 & 95 & 0 & 0\end{pmatrix}^T$
$\mathbf{m}_2$	$\begin{pmatrix}-6 & 95 & 0 & 0\end{pmatrix}^T$
$\mathbf{m}_3$	$\begin{pmatrix}-5 & 99 & 0 & 0\end{pmatrix}^T$
$\mathbf{m}_4$	$\begin{pmatrix}-8 & 95 & 0 & -1\end{pmatrix}^T$
P	$\text{diag}[\begin{pmatrix}1 & 1 & 0.1 & 0.1\end{pmatrix}^2]$
v	20
V	$\begin{pmatrix}0.5 & 0\\ 0 & 0.5\end{pmatrix}$
q	0.1
η	4
τ	10

3.2 **approach**

GGIW birth initial parameters	
Parameter	**Value**
α	8
β	2
$\mathbf{m}_1$	$\begin{pmatrix}-9.5 & 95 & 0 & 0\end{pmatrix}^T$
$\mathbf{m}_2$	$\begin{pmatrix}-6 & 95 & 0 & 0\end{pmatrix}^T$
$\mathbf{m}_3$	$\begin{pmatrix}-5 & 99 & 0 & 0\end{pmatrix}^T$
$\mathbf{m}_4$	$\begin{pmatrix}-8 & 95 & 0 & -1\end{pmatrix}^T$
P	$\text{diag}[\begin{pmatrix}1 & 1 & 0.1 & 0.1\end{pmatrix}^2]$
v	20
V	Shown in the main text
q	0.1
η	4
τ	10

4^{th} approach

GGIW birth initial parameters	
Parameter	**Value**
α	8
β	2
$\mathbf{m}_1$	$\begin{pmatrix}-7 & 97 & 0 & 0\end{pmatrix}^T$
$\mathbf{m}_2$	$\begin{pmatrix}-7 & 97 & 0 & 0\end{pmatrix}^T$
$\mathbf{m}_3$	$\begin{pmatrix}-7 & 97 & 0 & 0\end{pmatrix}^T$
$\mathbf{m}_4$	$\begin{pmatrix}-7 & 97 & 0 & -1\end{pmatrix}^T$
P	$\text{diag}[\begin{pmatrix}2 & 2 & 0.1 & 0.1\end{pmatrix}^2]$
v	20
V	Shown in the main text
q	0.1
η	4
τ	10